Electronic Supporting Information

Eight-Coordinate Mono- and Dinuclear Dy(III) Complexes Containing a Rigid equatorial plane and an Anisobidentate Carboxylate ligand in the Axial position: Synthesis, Structure and Magnetism.

Pankaj Kalita*,[a] Kusum Kumari,[b] Pawan Kumar,[c] Vierandra Kumar,[c] Saurabh Kumar Singh,*[b] Guillaume Rogez*[d] and Vadapalli Chandrasekhar*[c]

[a]Department of Chemistry, Nowgong Girls' College, Nagaon, Assam-782 002, India.

[b]Department of Chemistry, Indian Institute of Technology Hyderabad, Kandi, Sangareddy, Telangana-502 285, India.

[c]Tata Institute of Fundamental Research Hyderabad, Gopanpally, Hyderabad-500 107, India.

[d]Institut de Physique et Chimie des Matériaux de Strasbourg (IPCMS) CNRS/Université de Strasbourg, UMR 7504, 67000 Strasbourg, France.

*vc@tifr.res.in; Guillaume.Rogez@ipcms.unistra.fr; sksingh@chy.iith.ac.in;

pankajkalita976@gmail.com

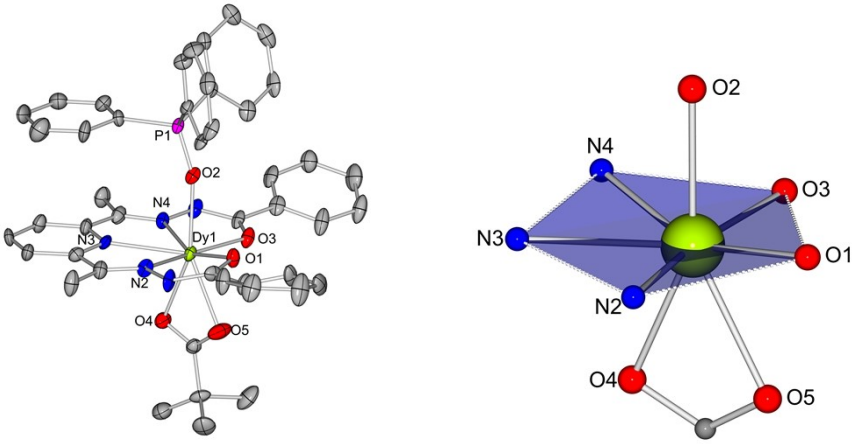

Figure S1. Molecular structure of complex **2**. Thermal ellipsoids at 30% probability level are shown (*left*) and the hula-hoop like coordination geometry (*right*). (The H atoms, disordered atoms and masked solvent molecules are removed for clarity)

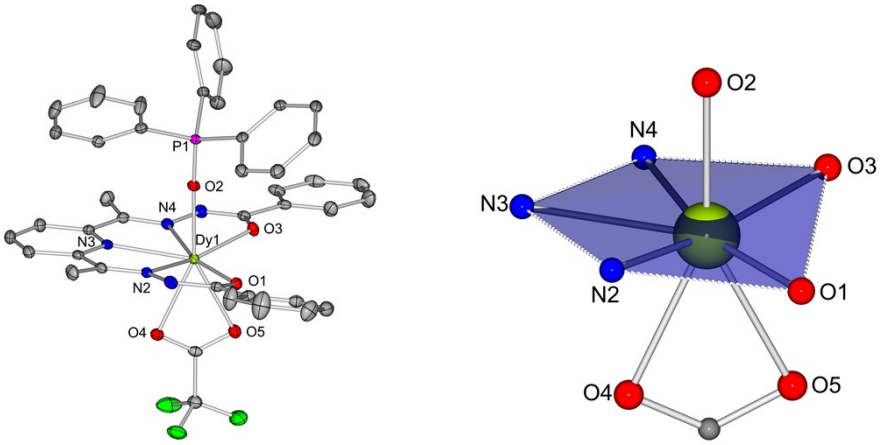

Figure S2. Molecular structure of complex **3**. Thermal ellipsoids at 30% probability level are shown (*left*) and the hula-hoop like coordination geometry (*right*). (The H atoms are removed for clarity)

Table S1. The average *enolate* and *imino* bond lengths of $[L]^{2-}$ and Dy−O_{phos} distances

Complex	**C=N (Å)**	**C−O (Å)**	**Dy–O_{phos} (Å)**	**Ref.**
(L′)$DyCl_2$	1.338	1.275	–	[1]
[(L)Dy(Cy_3PO)Cl]	1.322	1.289	2.237	[2]
[(L)Dy(Ph_3PO)Cl]	1.327	1.287	2.276	[2]
[(L)Dy($Cy_3PO)_2$]	1.325	1.283	2.231	[3]
Complex **1**	1.323	1.281	2.280	This work
Complex **2**	1.338	1.287	2.307	
Complex **3**	1.325	1.284	2.281	
Complex **4**	1.325	1.285	2.308	

(Typical bond lengths of C=N: 1.29 Å; Csp^2–Nsp^3: 1.43 Å; C=O: 1.21 Å; Csp^2–O: 1.35 Å)

Table S2. Analysis of Dy(III) coordination geometry using SHAPE.

Complex	Structure†												
	OP-8	HPY-8	HBPY-8	CU-8	SAPR-8	**TDD-8**	JGBF-8	JETBPY-8	JBTPR-8	**BTPR-8**	JSD-8	TT-8	ETBPY-8
Complex 1	32.509	22.252	10.799	9.832	6.149	**4.789**	9.435	23.747	5.298	**4.594**	6.082	10.654	20.796
Complex 2	32.731	22.412	12.814	11.370	5.561	**3.752**	10.104	23.106	5.025	**4.352**	5.050	12.133	20.028
Complex 3	33.868	23.446	11.026	9.956	5.244	**4.611**	8.806	25.957	5.138	**4.424**	5.857	10.744	22.730
Complex 4	32.063	21.771	14.585	13.305	5.987	**3.958**	11.021	22.905	4.371	**3.627**	5.250	13.971	19.359

†OP-8: Octagon (D_{8h}); HPY-8: Heptagonal pyramid (C_{7v}); HBPY-8: Hexagonal bipyramid (D_{6h}); CU-8 Cube (O_h); SAPR-8: Square antiprism (D_{4d}); TDD-8: Triangular dodecahedron (D_{2d}); JGBF-8: Johnson gyrobifastigium J26 (D_{2d}); JETBPY-8: Johnson elongated triangular bipyramid J14 (D_{3h}); JBTPR-8: Biaugmented trigonal prism J50 (C_{2v}); BTPR-8: Biaugmented trigonal prism (C_{2v}); JSD-8 Snub diphenoid J84 (D_{2d}); TT-8: Triakis tetrahedron (T_d) ETBPY-8: Elongated trigonal bipyramid (D_{3h})

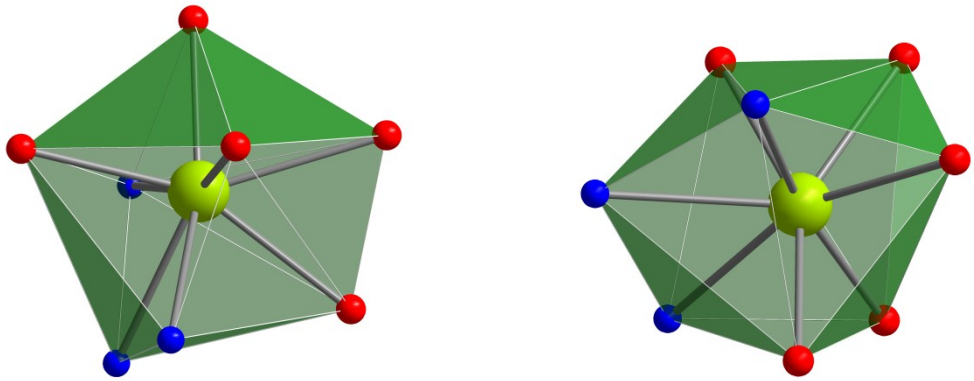

Figure S3. The triangular dodecahedron (TDD-8; *left*) and the biaugmented trigonal prism (BTPR-8; *right*) coordination geometries of the Dy(III) in complex **1**.

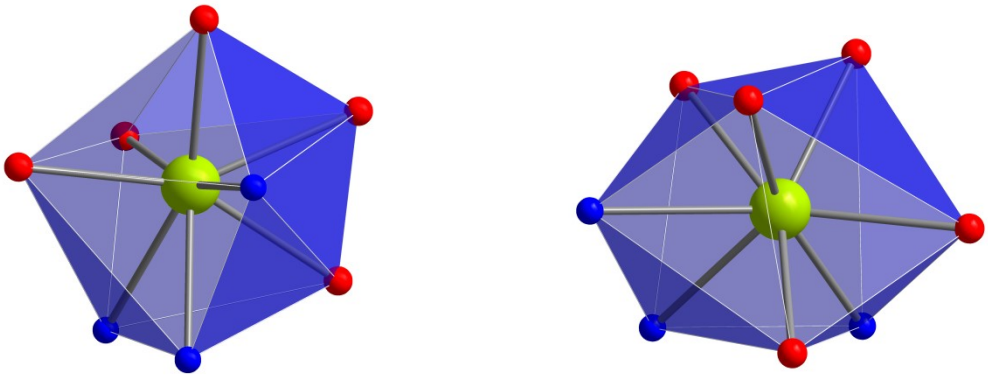

Figure S4. The triangular dodecahedron (TDD-8; *left*) and the biaugmented trigonal prism (BTPR-8; *right*) coordination geometries of the Dy(III) in complex **2**.

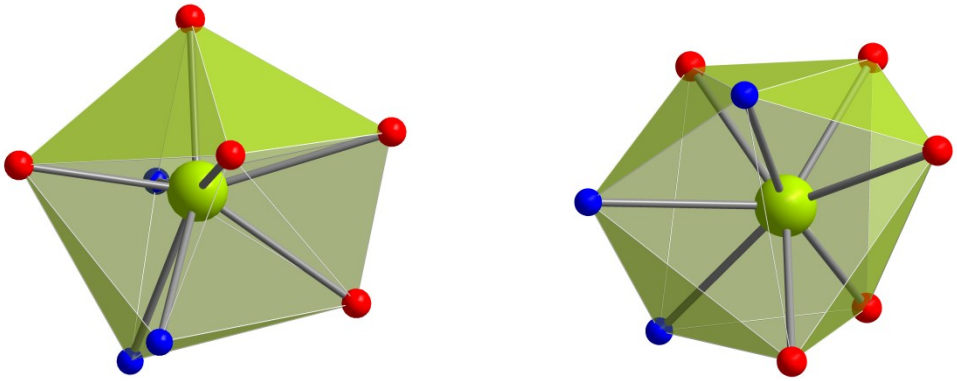

Figure S5. The triangular dodecahedron (TDD-8; *left*) and the biaugmented trigonal prism (BTPR-8; *right*) coordination geometries of the Dy(III) in complex **3**.

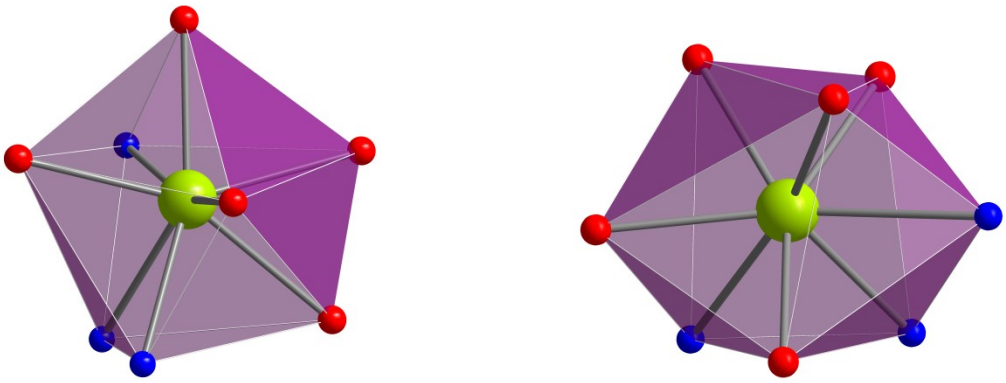

Figure S6. The triangular dodecahedron (TDD-8; *left*) and the biaugmented trigonal prism (BTPR-8; *right*) coordination geometries of the Dy(III) in complex **4**.

Table S3. Crystallographic details of complexes **2**–**4**.

Bond distances (Å)		**Bond angles (°)**			
Complex 2		O1−Dy1−O4	124.7(4)	O1−Dy1−O5	73.2(4)
		O1−Dy1−N2	64.0(3)	O1−Dy1−N3	126.3(4)
		O1−Dy1−N4	157.3(4)	O2−Dy1−O1	80.3(3)
Dy1−O1	2.329(9)	O2−Dy1−O4	154.5(3)	O2−Dy1−O5	151.6(4)
Dy1−O2	2.307(8)	O2−Dy1−N2	89.1(3)	O2−Dy1−N3	85.5(3)
Dy1−O3	2.287(9)	O2−Dy1−N4	80.8(3)	O3−Dy1−O1	101.1(3)
Dy1−O4	2.419(9)	O3−Dy1−O2	86.4(3)	O3−Dy1−O4	92.7(3)
Dy1−O5	2.390(1)	O3−Dy1−O5	88.7(4)	O3−Dy1−N2	165.0(3)
Dy1−N2	2.448(8)	O3−Dy1−N3	129.5(4)	O3−Dy1−N4	65.2(3)
Dy1−N3	2.463(1)	O4−Dy1−N2	97.4(4)	O4−Dy1−N3	75.4(3)
Dy1−N4	2.464(9)	O4−Dy1−N4	75.7(3)	O5−Dy1−O4	53.6(4)
		O5−Dy1−N2	88.5(4)	O5−Dy1−N3	118.5(5)
		O5−Dy1−N4	121.9(3)	N2−Dy1−N3	64.2(4)
		N2−Dy1−N4	128.1(3)	N3−Dy1−N4	64.4(3)
Complex 3		O1−Dy1−O2	86.91(8)	O1−Dy1−O3	101.38(7)

		O1−Dy1−O4	99.61(8)	O1−Dy1−O5	78.29(8)
		O1−Dy1−N2	65.08(8)	O1−Dy1−N3	129.12(8)
Dy1−O1	2.276(2)	O1−Dy1−N4	165.82(8)	O2−Dy1−O3	85.04(8)
Dy1−O2	2.281(2)	O2−Dy1−O4	153.65(7)	O2−Dy1−O5	153.01(7)
Dy1−O3	2.300(2)	O2−Dy1−N2	77.93(8)	O2−Dy1−N3	83.22(7)
Dy1−O4	2.461(2)	O2−Dy1−N4	89.80(8)	O3−Dy1−O4	118.07(7)
Dy1−O5	2.512(2)	O3−Dy1−O5	76.06(8)	O3−Dy1−N2	158.55(8)
Dy1−N2	2.467(2)	O3−Dy1−N3	127.06(8)	O3−Dy1−N4	64.56(8)
Dy1−N3	2.491(2)	O4−Dy1−O5	52.63(7)	O4−Dy1−N2	81.76(8)
Dy1−N4	2.457(3)	O4−Dy1−N3	72.82(7)	N2− Dy1−O5	114.75(8)
		N2−Dy1−N3	64.04(8)	N3−Dy1−O5	123.58(7)
		N4−Dy1−O4	89.41(8)	N4−Dy1−O5	99.03(8)
		N4−Dy1−N2	127.57(8)	N4−Dy1−N3	63.97(8)
Complex 4		O1−Dy1−O2	100.30(10)	O1−Dy1−O3	87.47(11)
		O1−Dy1−O4	90.12(11)	O1−Dy1−O5	94.56(11)
		O1−Dy1−N2	65.20(10)	O1−Dy1−N3	129.08(10)
Dy1−O1	2.288(3)	O1−Dy1−N4	164.27(10)	O2−Dy1−O3	79.16(10)
Dy1−O2	2.307(3)	O2−Dy1−O4	126.48(10)	O2−Dy1−O5	73.25(10)
Dy1−O3	2.308(3)	O2−Dy1−N2	155.50(11)	O2−Dy1−N3	127.28(10)
Dy1−O4	2.442(3)	O2−Dy1−N4	64.69(10)	O3−Dy1−O4	154.20(10)
Dy1−O5	2.417(3)	O3−Dy1−O5	152.26(11)	O3−Dy1−N2	80.50(11)
Dy1−N2	2.466(3)	O3−Dy1−N3	85.17(11)	O3−Dy1−N4	85.07(11)
Dy1−N3	2.487(3)	O4−Dy1−N2	75.20(10)	O4−Dy1−N3	76.51(11)
Dy1−N4	2.469(3)	O4−Dy1−N4	102.55(11)	O5−Dy1−O4	53.55(10)
		O5−Dy1−N2	125.33(10)	O5−Dy1−N3	113.90(11)
		O5−Dy1−N4	85.78(12)	N2−Dy1−N3	63.88(11)
		N2−Dy1−N4	126.77(11)	N4−Dy1−N3	64.02(11)

Table S4. Analysis of short ring-interactions with Cg-Cg distances < 5.0 Å, Alpha < 20.00º and Beta < 60.00º for **1**.

[ARU(J)] = Symmetry operation on Cg(J)

Alpha = Dihedral Angle between Planes I and J (Deg)

Beta = Angle Cg(I) > Cg(J) or Cg(I) > Me vector and normal to plane I (Deg)

Gamma = Angle Cg(I) >Cg(J) vector and normal to plane J (Deg)

Cg-Cg = Distance between ring Centroids (Ang.)

CgI_Perp = Perpendicular distance of Cg(I) on ring J (Ang.)

CgJ_Perp = Perpendicular distance of Cg(J) on ring I (Ang.)

Slippage = Distance between Cg(I) and Perpendicular Projection of Cg(J) on Ring I (Ang).

Cg(I)	Cg(J)	[ARU(J)]	Cg-Cg	Alpha	Beta	Gamma	CgI_Perp	CgJ_Perp	Slippage
Cg1	Cg7	X,Y,Z	3.8201(15)	9.51(13)	17.7	27.2	3.3983(11)	3.6399(11)	1.160
Cg1	Cg8	-/2+X,1/2-Y,-1/2+Z	4.6757(15)	15.51(12)	40.2	55.1	2.6759(11)	3.5728(11)	3.016
Cg5	Cg5	1-X,1-Y,-Z	4.9925(16)	0.02(13)	50.8	50.8	3.1522(11)	3.1523(11)	3.871

Cg1: (N3, C3, C4, C5, C6, C7); Cg5: (C25, C26, C27, C28, C29, C30); Cg7: (C37, C38, C39, C40, C41, C42); Cg8: (C43, C44, C45, C46, C47, C48)

Table S5. Analysis of X-H···Cg (Pi-ring) interactions (H···Cg < 3.0 Å, Gamma < 40.0º) for **1**.

Cg(J) = Center of gravity of ring J (Plane number above)

[ARU(J)] = Symmetry operation on Cg(J)

H-Perp = Perpendicular distance of H to ring plane J

Gamma = Angle between Cg-H vector and ring J normal

X–H…Cg = X-H-Cg angle (degrees)

X…Cg = Distance of X to Cg (Angstrom)

X–H, Pi = Angle of the X-H bond with the Pi-plane (i.e.' Perpendicular = 90 degrees, Parallel = 0 degrees)

X–H(I)	Cg(J)	[ARU(J)]	H…Cg	H-Perp	Gamma	X–H..Cg	X..Cg	X–H, Pi
C28–H28	Cg8	3/2-X,1/2+Y, 1/2-Z	2.63	-2.59	9.95	148	3.473(3)	67
C15–H15	Cg6	1+X, Y, Z	2.91	-2.91	3.04	148	3.755(3)	61
C26–H26	Cg2	-1/2+X,1/2-Y, -1/2+Z	2.98	-2.82	18.87	150	3.835(3)	54
C35–H35	Cg5	-1/2+X,1/2-Y,1/2+Z	3.00	2.71	25.26	139	3.768(3)	44

Cg2: (C12, C13, C14, C15, C16, C17); Cg5: (C25, C26, C27, C28, C29, C30); Cg6: (C31, C32, C33, C34, C35, C36); Cg8: (C43, C44, C45, C46, C47, C48)

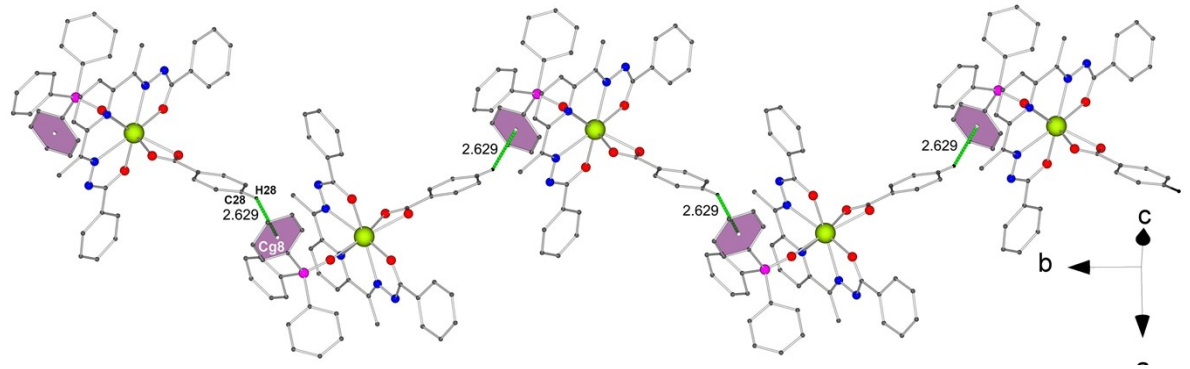

C28–H28···Cg8 interaction

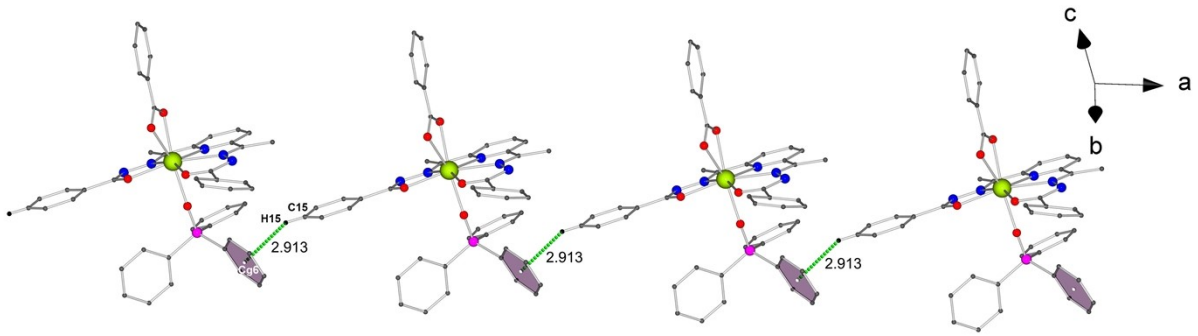

C15–H15···Cg6 interaction

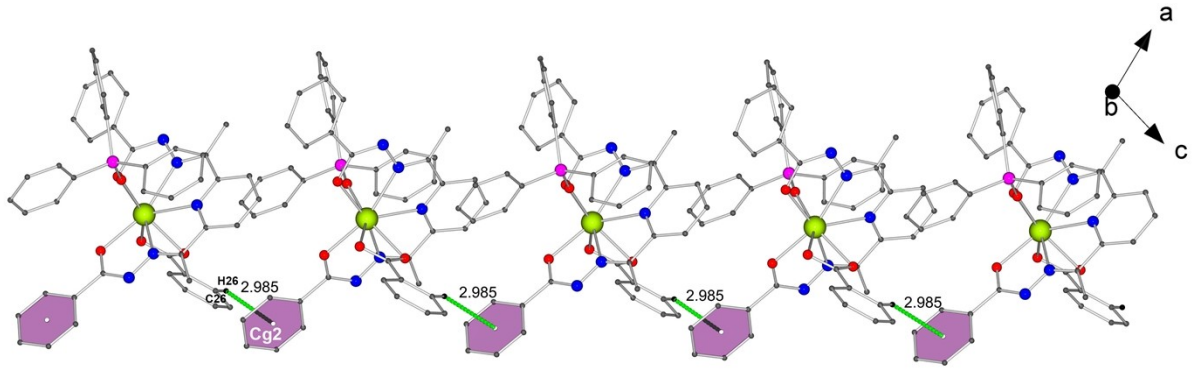

C26–H26···Cg2 interaction

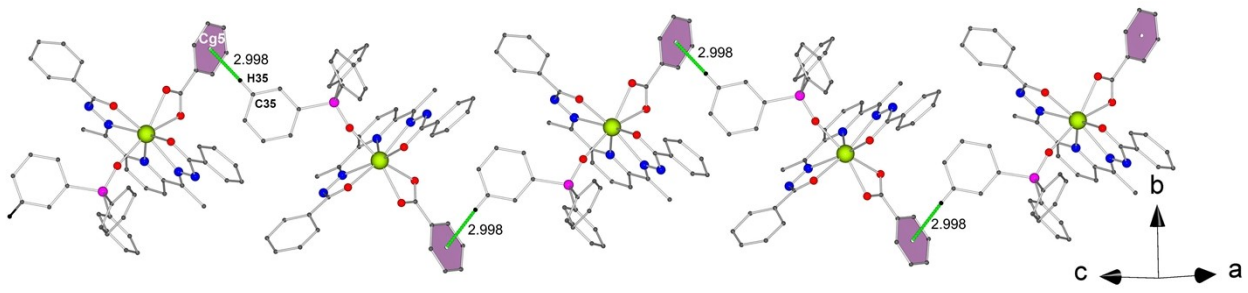

C35–H35···Cg5 interaction

Figure S7. Illustrations of different intermolecular X-H···Cg (Pi-Ring) interactions present in complex **1** (H-atoms except selected are omitted for clarity).

Table S6. Analysis of short ring-interactions with Cg-Cg distances < 5.0 Å, Alpha < 20.00º and Beta < 60.00º for **2**.

Cg(I)	Cg(J)	[ARU(J)]	Cg-Cg	Alpha	Beta	Gamma	CgI_Perp	CgJ_Perp	Slippage
Cg1	Cg6	X,Y,Z	3.565(10)	3.4(8)	17.9	18.7	3.377(6)	3.393(7)	1.093

Cg1: (N3, C3, C4, C5, C6, C7); Cg6: (C35, C36, C37, C38, C39, C40)

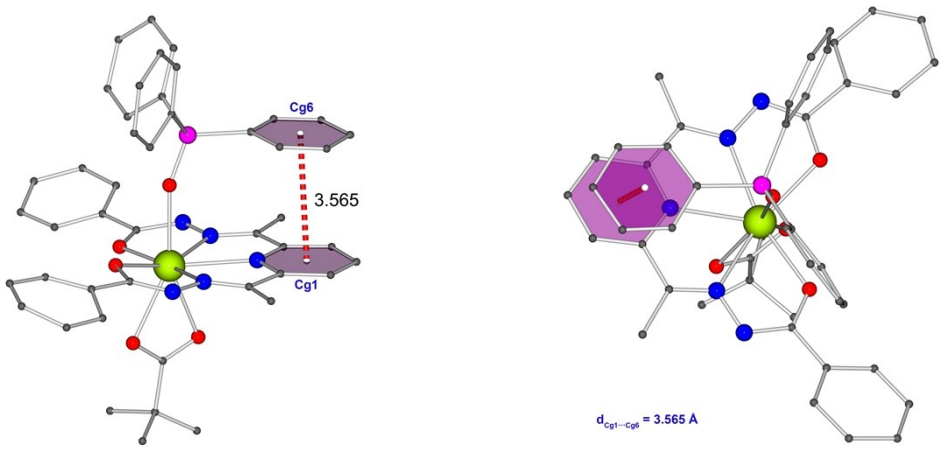

(*side view*) (*top view*)

Figure 8. Illustrations of intramolecular π···π ($d_{Cg1\cdots Cg6}$ = 3.565 Å) stacking interaction in complex **2** (H-atoms are omitted for clarity).

Table S7. Analysis of X-H···Cg (Pi-ring) interactions (H···Cg < 3.0 Å, Gamma < 40.0º) for **2**.

X–H(I)	Cg(J)	[ARU(J)]	H…Cg	H-Perp	Gamma	X–H..Cg	X..Cg	X–H, Pi
C27–H27B	Cg6	1/2+X,3/2-Y,-1/2+Z	2.59	-2.55	9.66	128	3.28(2)	48
C49–H49 (C15–H15)	Cg7	X,2-Y,-1/2+Z	2.90 (2.70)	2.82 (2.67)	13.48 (8.47)	156 (161)	3.78(3) (3.61(7))	69 (48)
C17–H17	Cg1	-1/2+X,3/2-Y,-1/2+Z	2.98	2.71	24.58	148	3.819(17)	43

Cg1: (N3, C3, C4, C5, C6, C7); Cg6: (C35, C36, C37, C38, C39, C40); Cg7: (C41, C42, C43, C44, C45, C46)

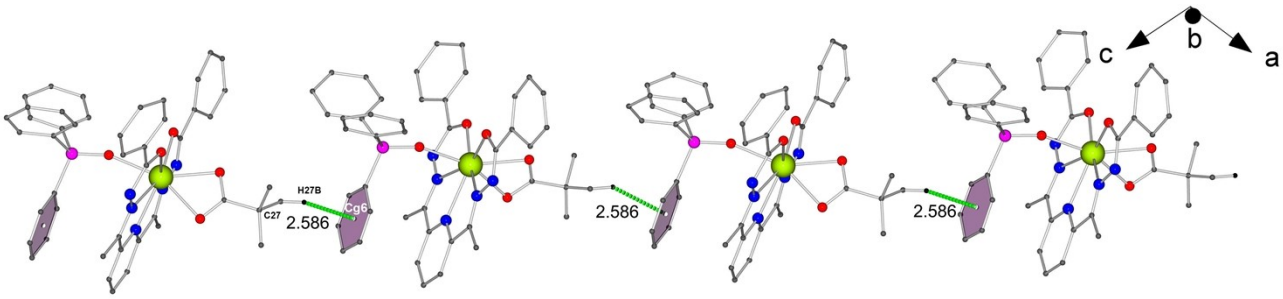

C27–H27B···Cg6 interaction

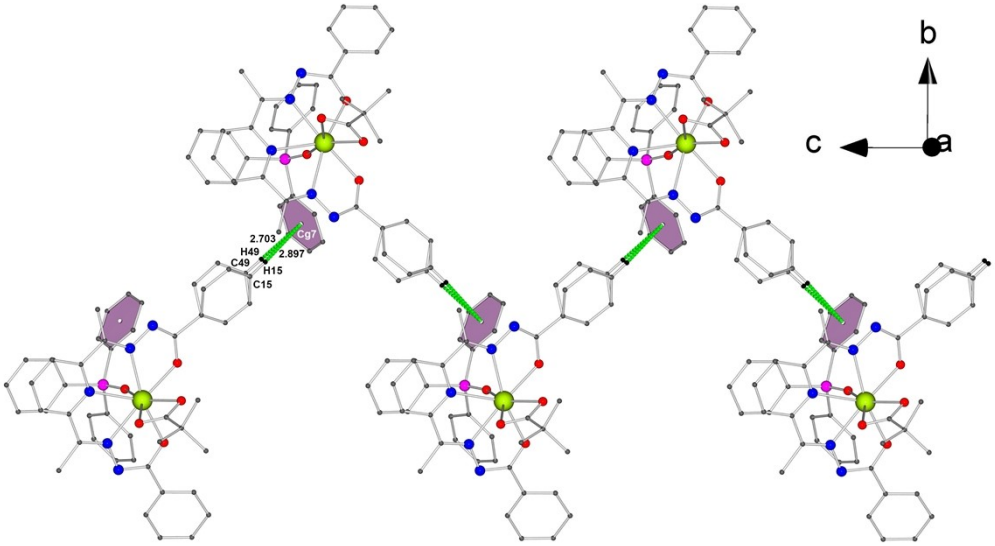

C49(C15)–H49(H15) ···Cg7 interaction

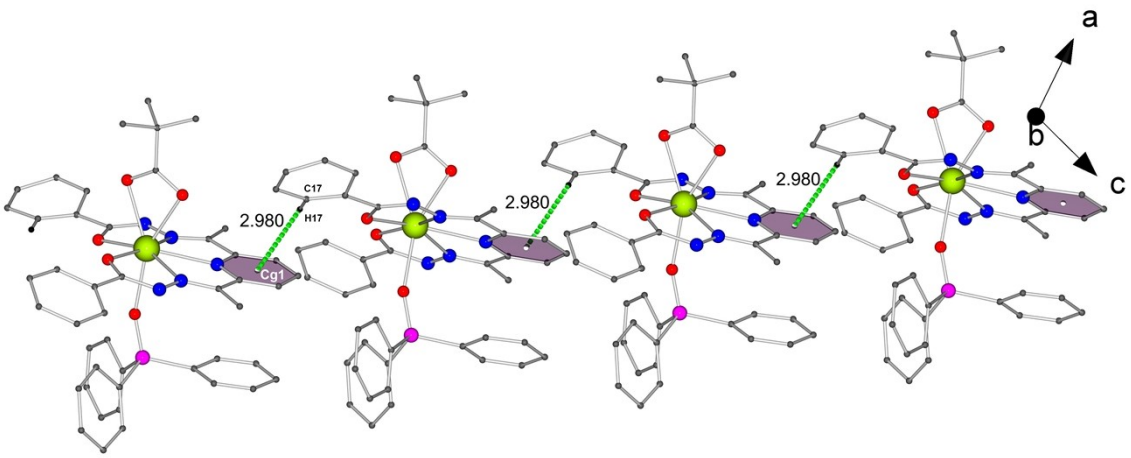

C17–H17···Cg1 interaction

Figure S9. Illustrations of different intermolecular C-H···Cg (Pi-ring) interactions present in complex **2** (All the H-atoms except selected are omitted for clarity).

Table S8. Analysis of short ring-interactions with Cg-Cg distances < 5.0 Å, Alpha < 20.00º and Beta < 60.00º for **3**.

Cg(I)	Cg(J)	[ARU(J)]	Cg-Cg	Alpha	Beta	Gamma	CgI_Perp	CgJ_Perp	Slippage
Cg1	Cg3	1-X,1-Y,-Z	4.238(2)	3.47(17)	36.6	39.0	3.2954(13)	3.4033(16)	2.526
Cg6	Cg6	1-X,1-Y,1-Z	3.673(2)	0.0(2)	25.6	25.6	-3.3127(17)	-3.3127(17)	1.586

Cg1: (N3, C3, C4, C5, C6, C7); Cg3: (C18, C19, C20, C21, C22, C23); Cg6: (C38, C39, C40, C41, C42, C43)

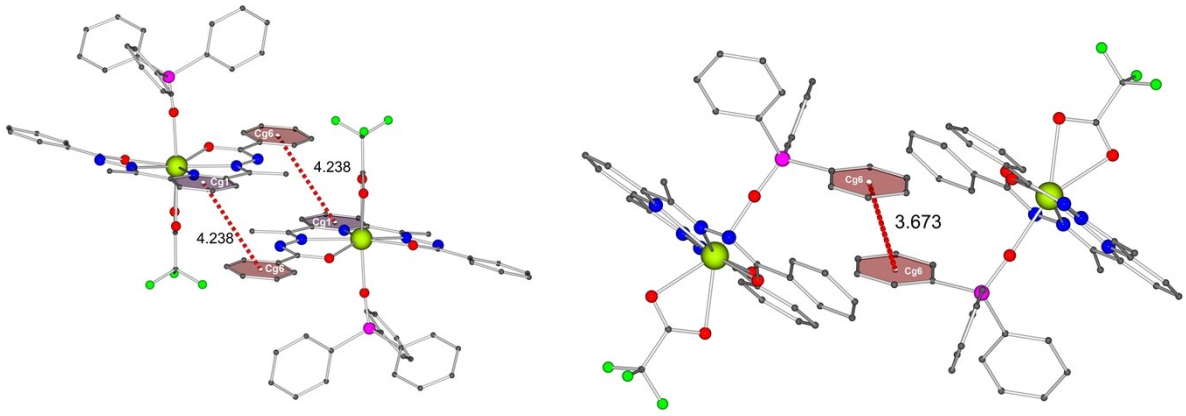

Figure S10. Illustrations of intramolecular π···π ($d_{Cg1\cdots Cg6}$ = 4.238 Å (*left*) and $d_{Cg6\cdots Cg6}$ = 3.673Å (*right*)) stacking interaction in complex **3** (H-atoms are omitted for clarity).

Table S9. Analysis of X-H···Cg (Pi-ring) interactions (H···Cg < 3.0 Å, Gamma < 40.0º) for **3**.

X–H(I)	Cg(J)	[ARU(J)]	H…Cg	H-Perp	Gamma	X–H..Cg	X..Cg	X–H, Pi
C11–H11A	Cg3	X,1+Y,Z	2.86	-2.75	16.18	130	3.555(4)	47

Cg3: (C18, C19, C20, C21, C22, C23)

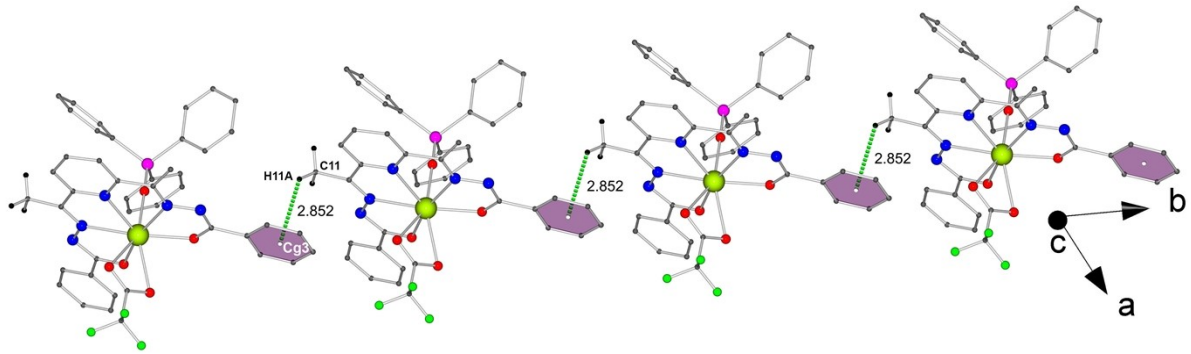

C11–H11A···Cg3 interaction

Figure S11. Illustrations of different intermolecular C-H···Cg (Pi-ring) interactions present in complex **3** (All the H-atoms except selected are omitted for clarity).

Table S10. Analysis of short ring-interactions with Cg-Cg distances < 5.0 Å, Alpha < 20.00º and Beta < 60.00º for **4**.

Cg(I)	Cg(J)	[ARU(J)]	Cg-Cg	Alpha	Beta	Gamma	CgI_Perp	CgJ_Perp	Slippage
Cg1	Cg6	X,Y,Z	3.821(3)	6.3(2)	20.7	26.9	-3.4064(18)	3.575(2)	1.350
Cg1	Cg2	1-X,1-Y,-Z	4.251(3)	2.3(2)	37.8	39.3	-3.2883(18)	-3.358(2)	2.606
Cg3	Cg3	-X,-Y,1-Z	4.849(3)	0.0(2)	40.2	40.2	-3.701(2)	3.702(2)	3.132

Cg1: (N3, C3, C4, C5, C6, C7); Cg2: (C12, C13, C14, C15, C16, C17); Cg3: (C18, C19, C20, C21, C22, C23); Cg6: (C34, C35, C36, C37, C38, C39)

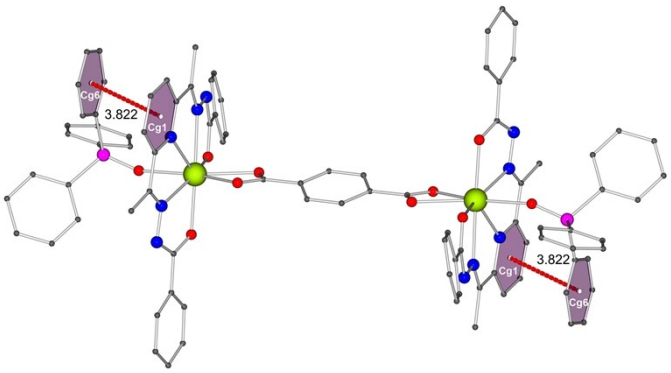

Figure S12. Illustration of intramolecular π···π ($d_{Cg1\cdots Cg6}$ = 3.822 Å) stacking interaction in complex **4** (H-atoms are omitted for clarity).

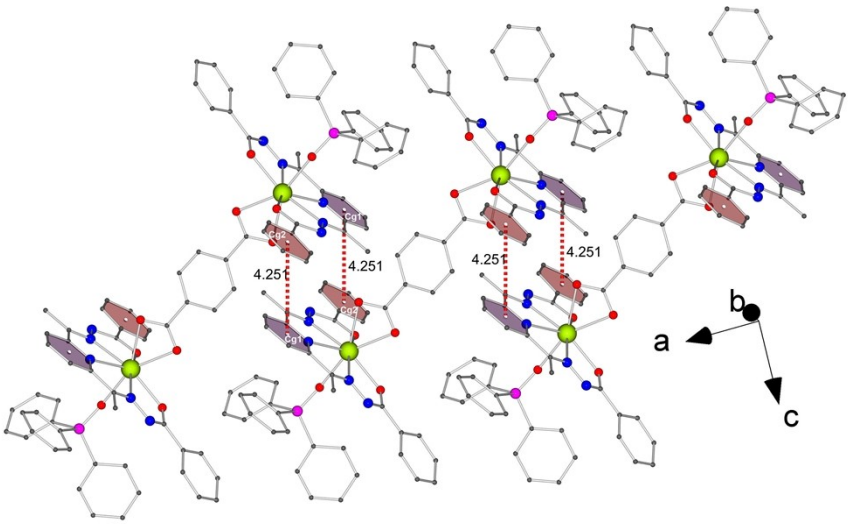

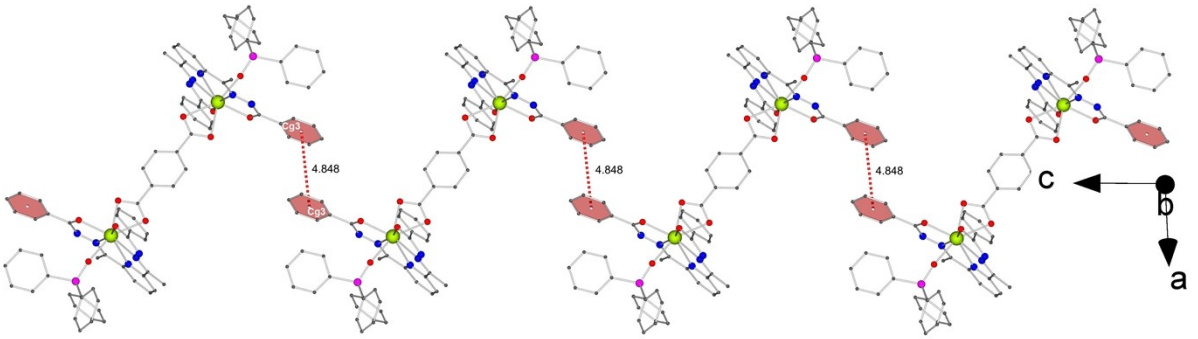

Figure S13. Illustrations of different intermolecular π···π ($d_{Cg1\cdots Cg2}$ = 4.251 Å (*top*) and $d_{Cg3\cdots Cg3}$ = 4.848 Å (*bottom*)) stacking interaction in complex **4**.

Table S11. Analysis of X-H···Cg (Pi-ring) interactions (H···Cg < 3.0 Å, Gamma < 40.0º) for **3**.

X–H(I)	Cg(J)	[ARU(J)]	H…Cg	H-Perp	Gamma	X–H..Cg	X..Cg	X–H, Pi
C5–H5	Cg4	1+X,Y,Z	2.83	-2.78	11.67	147	3.661(6)	60
C10–H10B	Cg2	X,-1+Y,Z	2.70	2.69	7.87	141	3.510(5)	54
C30–H30	Cg3	X,Y,Z	2.84	2.76	14.02	133	3.546(8)	49
C32–H32	Cg6	2-X,1-Y,1-Z	2.57	2.55	6.42	173	3.495(6)	79

Cg2: (C12, C13, C14, C15, C16, C17); Cg3: (C18, C19, C20, C21, C22, C23); Cg4: (C25, C26, C27, C28, C29, C30); Cg6: (C34, C35, C36, C37, C38, C39)

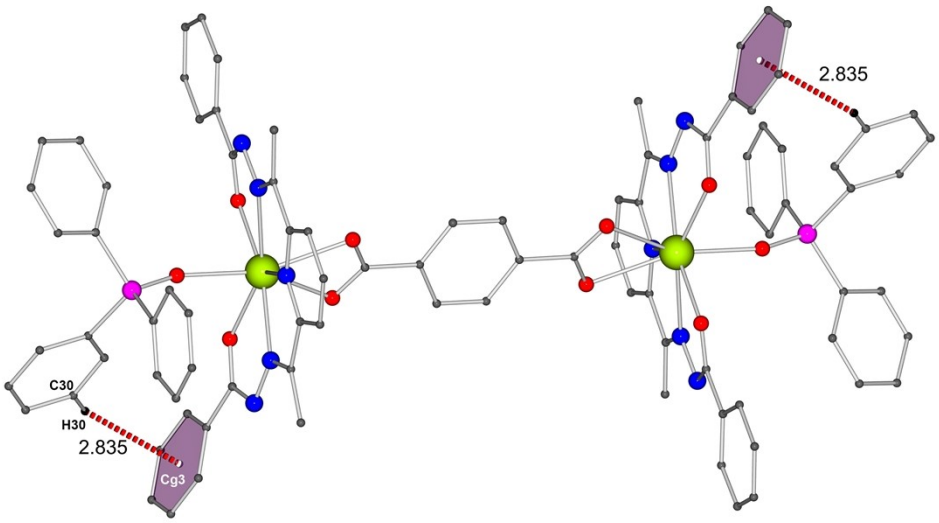

C30–H30···Cg3 interaction

Figure S14. Illustration of intramolecular C-H···Cg (Pi-ring) interactions present in complex **4** (All the H-atoms except selected are omitted for clarity).

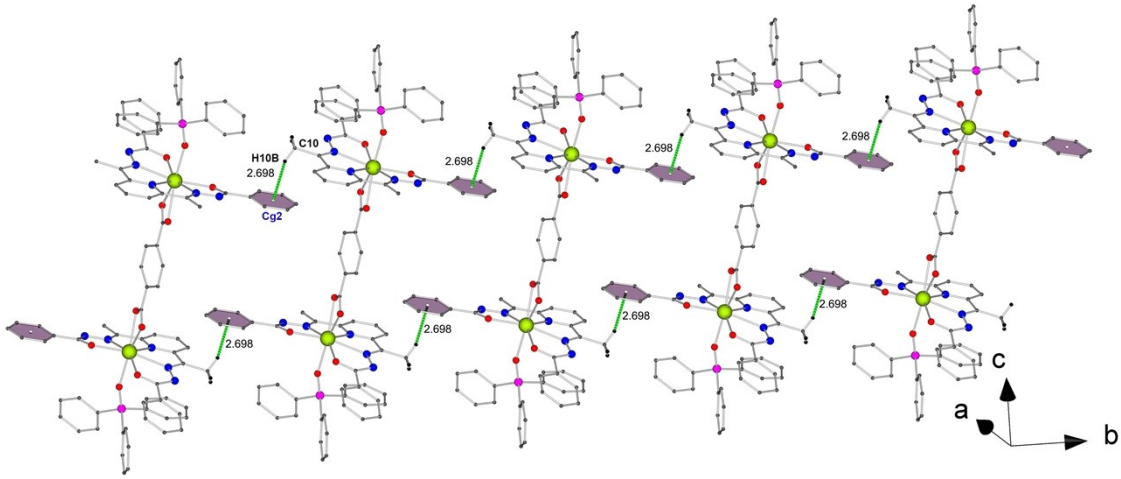

C10–H10B···Cg2 interaction

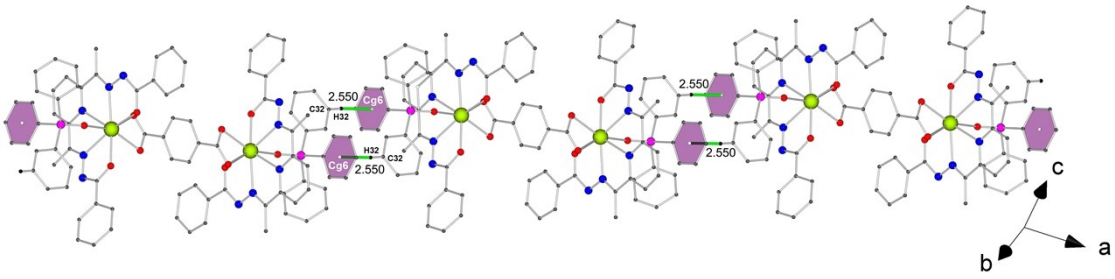

C32–H32···Cg6 interaction

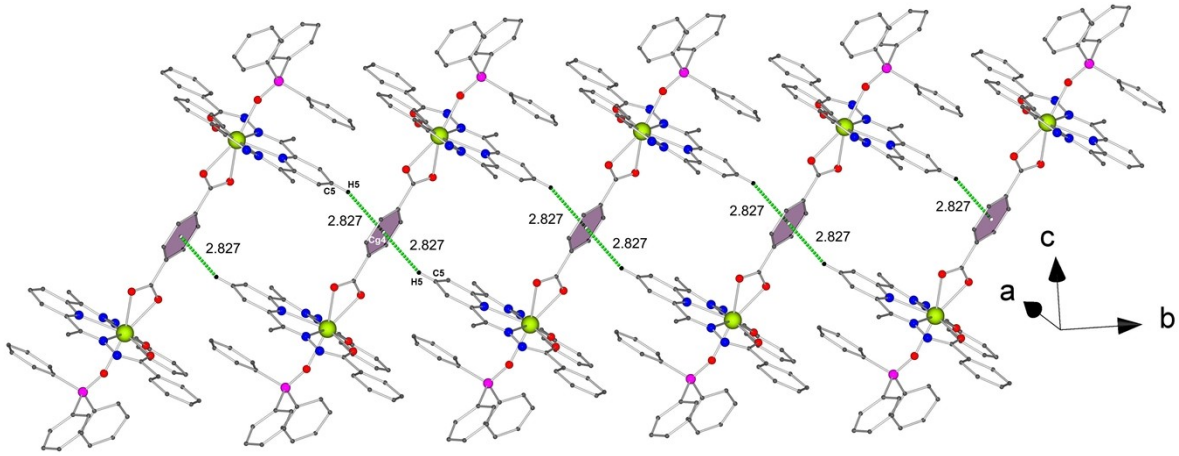

C5–H5···Cg4 interaction

Figure S15. Illustrations of different intermolecular C-H···Cg (Pi-ring) interactions present in complex **4** (All the H-atoms except selected are omitted for clarity).

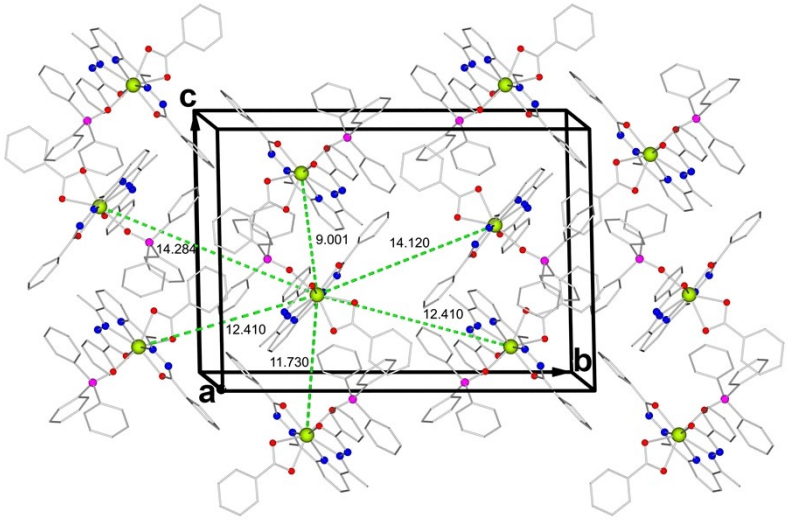

Figure S16. Solid-state packing diagram of complex **1** viewed along the crystallographic ***a*** axis. (H-atoms are omitted for clarity)

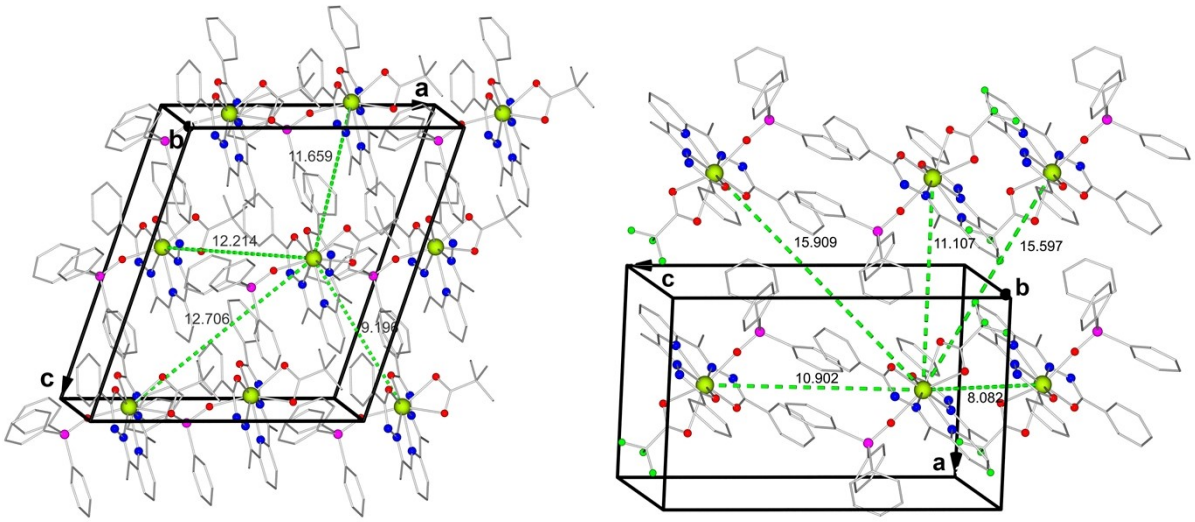

Figure S17. Solid-state packing diagram of complexes **2** (*left*) and **3** (*right*) viewed along the crystallographic ***b*** axis. (H-atoms are omitted for clarity)

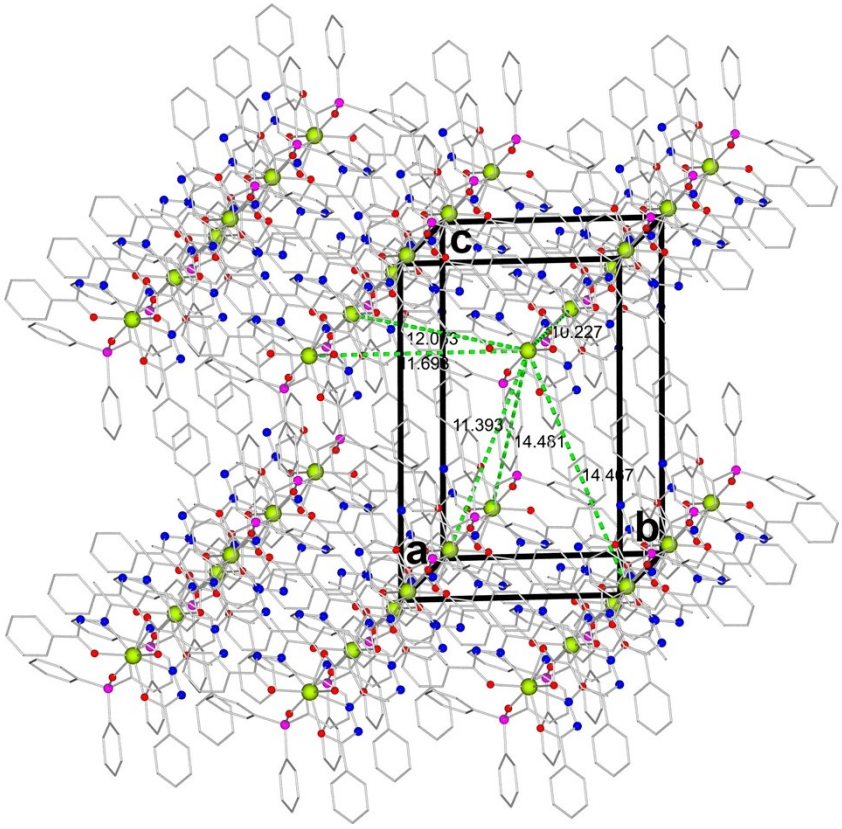

Figure S18. Solid-state packing diagram of complex **4** viewed along the crystallographic ***a*** axis. (H-atoms are omitted for clarity).

Electronic supporting information for the Magnetism section

For Complex 1

The low-temperature frequency-dependent ac susceptibility data for **1** were analyzed by using a generalized Debye model to fit the Cole–Cole plot (Figure S19):

$$\chi' = \chi_\infty + \frac{(\chi_0 - \chi_\infty)[1 + (2\pi\nu_{ac}\tau)^{1-\alpha}\sin(\frac{\alpha\pi}{2})]}{1 + 2(2\pi\nu_{ac}\tau)^{1-\alpha}\sin\left(\frac{\alpha\pi}{2}\right) + (2\pi\nu_{ac}\tau)^{2(1-\alpha)}}$$

$$\chi'' = \frac{(\chi_0 - \chi_\infty)(2\pi\nu_{ac}\tau)^{1-\alpha}\cos(\frac{\alpha\pi}{2})}{1 + 2(2\pi\nu_{ac}\tau)^{1-\alpha}\sin\left(\frac{\alpha\pi}{2}\right) + (2\pi\nu_{ac}\tau)^{2(1-\alpha)}}$$

where χ_∞ is the adiabatic susceptibility (at $\nu_{ac} \rightarrow \infty$), χ_0 is the isothermal susceptibility (at $\nu_{ac} \rightarrow 0$) and τ is the average relaxation time of magnetization.

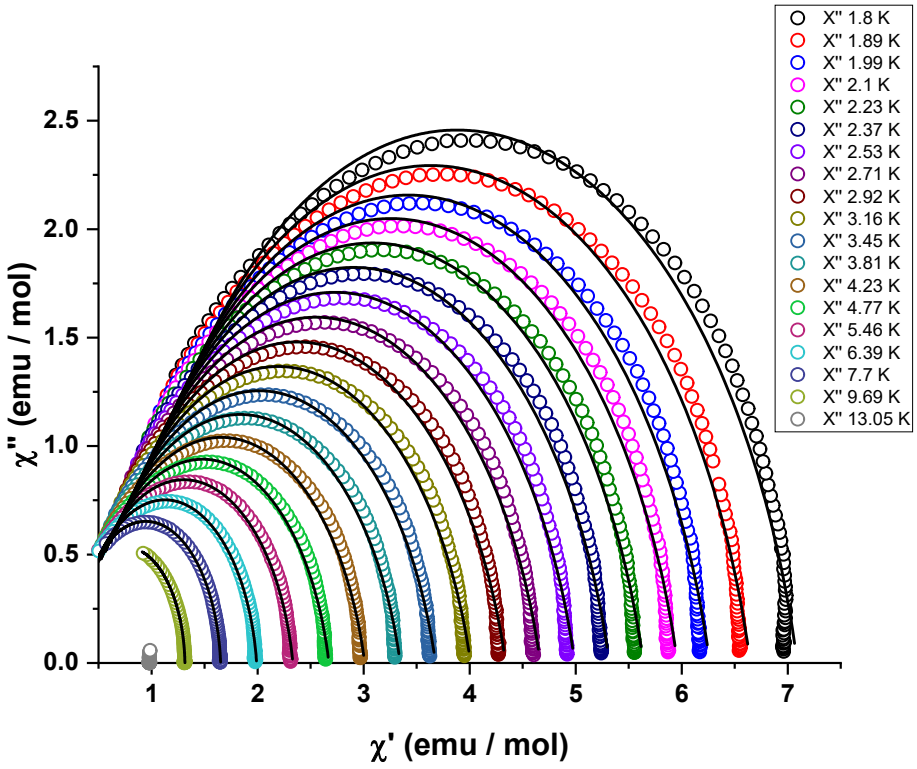

Figure S19. Cole–Cole plots for **1** at various temperatures and under an applied dc field of 0 Oe (open circles: experimental points, full lines: fits obtained with a generalized Debye model).

Although the fit is not perfect, likely due to a inhomogeneous distribution of the relaxation times, it provides satisfying parameters, collected in table S12 below:

Table S12. Parameters of the extended Debye model used to fit the Cole–Cole plots for **1** at various temperatures and under an applied dc field of 0 Oe.

T (K)	χ_0 (emu / mol)	χ_∞ (emu / mol)	τ (ms)	α
1.80	7.09094	0.67534	0.999084	0.16779
1.89	6.6479	0.61784	1.01	0.17207
1.99	6.26542	0.58107	1.01	0.17341
2.10	5.96107	0.55097	1.02	0.17465
2.23	5.63847	0.52789	1.02	0.17437
2.37	5.31978	0.49245	1.02	0.17618
2.53	4.99325	0.46305	1.02	0.17708
2.71	4.6679	0.43328	1.03	0.17836
2.92	4.33942	0.40593	1.02	0.17863
3.16	4.0089	0.37832	1.02	0.17829

3.45	3.67853	0.35181	1.00	0.17704
3.81	3.34529	0.32814	0.973896	0.17299
4.23	3.01125	0.30637	0.925244	0.16529
4.77	2.67337	0.28997	0.84289	0.15008
5.46	2.33327	0.2762	0.713188	0.12456
6.39	1.99119	0.26014	0.533501	0.08919
7.70	1.65149	0.23806	0.32552	0.050382
9.69	1.31463	0.21031	0.118634	0.02256

For Complex 2

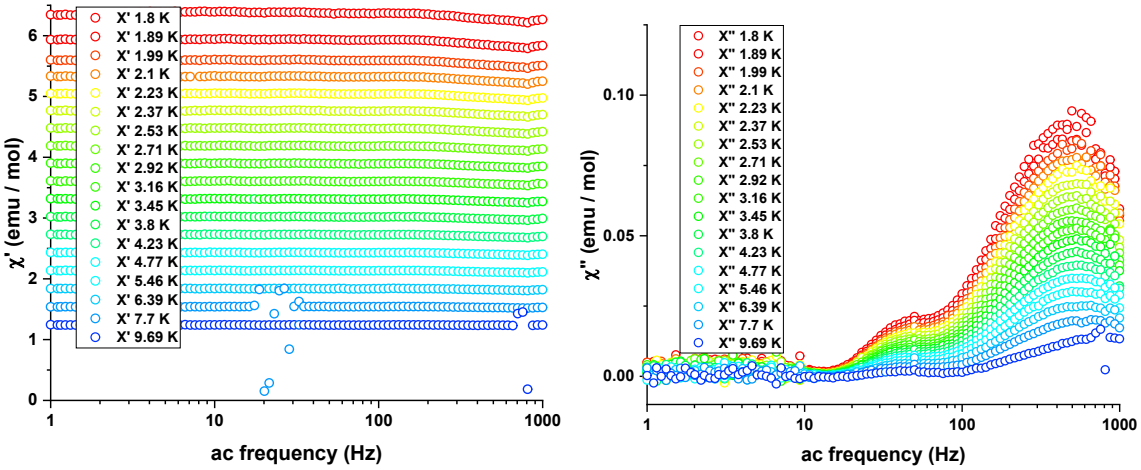

Figure S20. In-phase (*left*) and out-of-phase (*right*) susceptibility curves for complex **2** with an ac field of 2 Oe under a static dc field of 0 Oe at various temperatures.

The optimum field to reduce Quantum Tunneling of Magnetization for **2** was chosen as the one which provides the slowest magnetic relaxation. This determination was performed at 1.8 K (Figure S21).

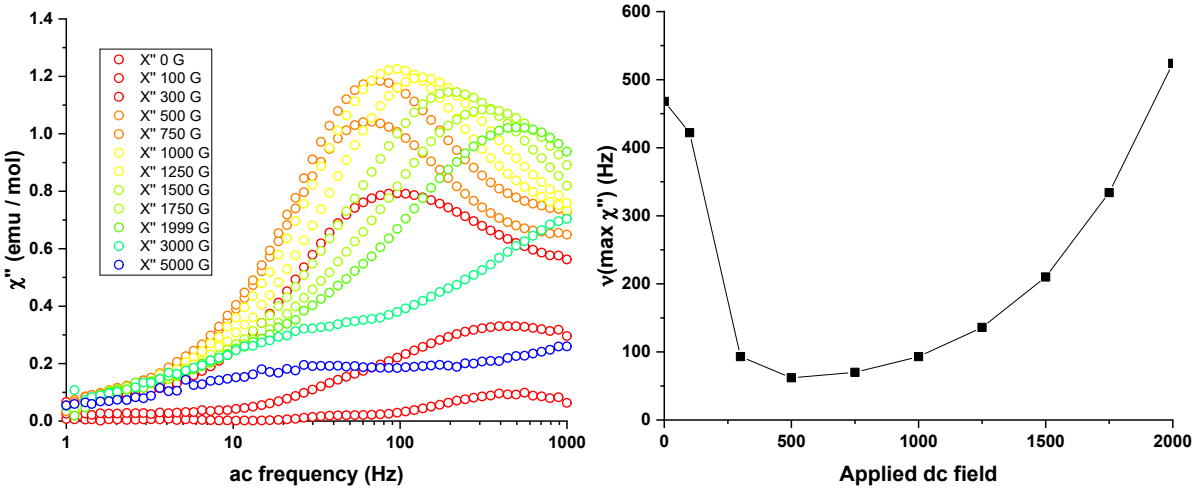

Figure S21. (left) out-of-phase susceptibility curves for complex **2** at 1.8 K with an ac field of 2 Oe and under various applied dc fields. (right) frequency of the maximum of χ″ as a function of the applied dc field at 1.8 K.

For **2**, the Cole-Cole plots (Figure S22) cannot be fitted by a generalized Debye model, likely due to a non-symmetrical distribution of the relaxation times. This asymmetry of the relaxation time distribution at 500 Oe can be due to the vicinity of different relaxation modes, difficult to separate from each-other, or to structural disorder.

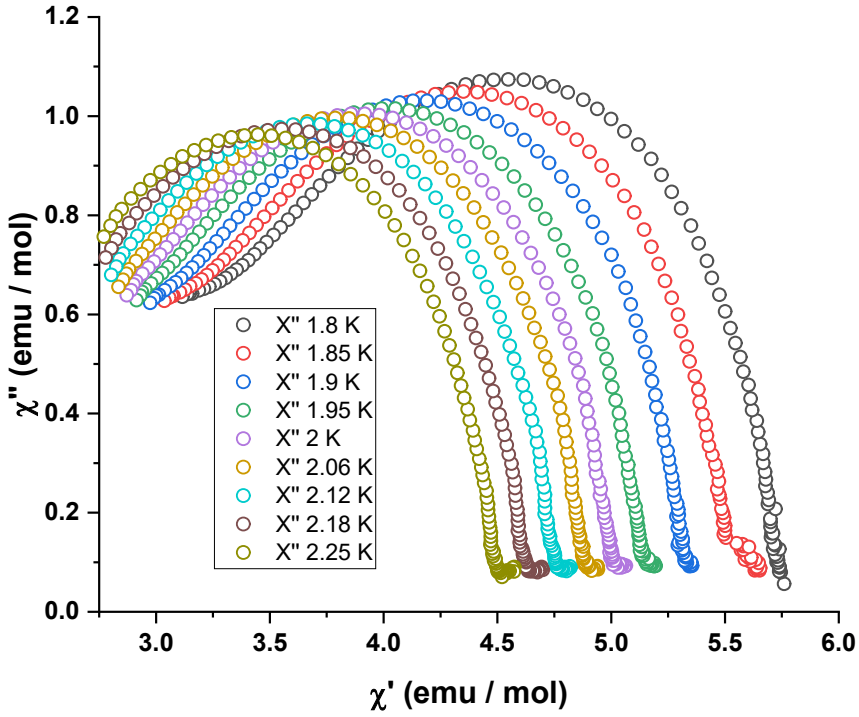

Figure S22. Cole-Cole plots for **2** under a static dc field of 500 Oe at various temperatures.

As a consequence, the relaxation times were determined manually, from the maxima of the χ" curves (Table S13):

Table S13. Relaxation times for **2** at various temperatures and under an applied dc field of 500 Oe.

T (K)	τ (×10^{-4} s)
1.80	24.2
1.85	19.9
1.90	15.6
1.95	12.5

2.00	10.1
2.06	8.48
2.12	6.89
2.18	5.59
2.25	4.53
2.32	3.50
2.40	2.75
2.49	2.16
2.58	1.70

For Complex 3

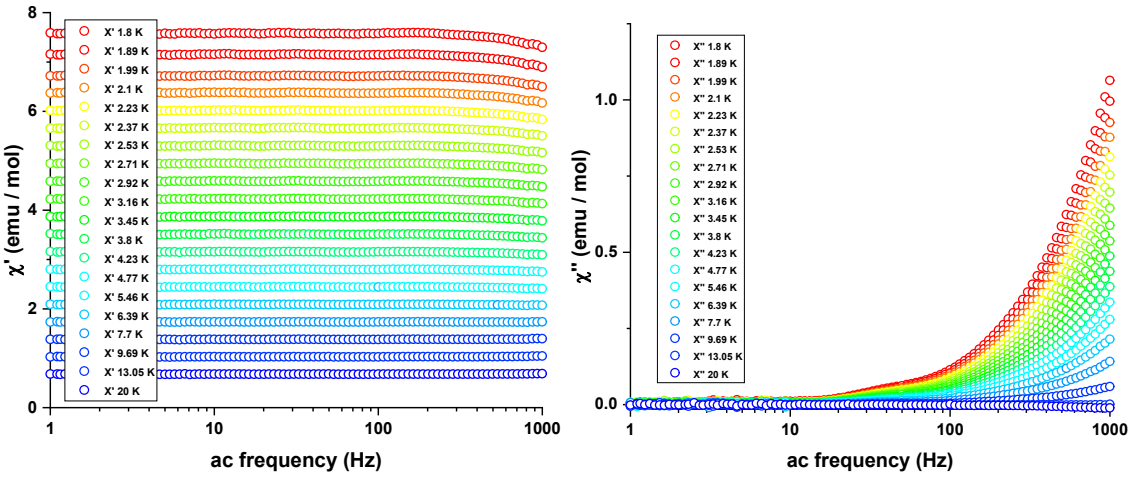

Figure S23. in-phase (*left*) and out-of-phase (*right*) susceptibility curves for complex **3** with an ac field of 2 Oe under a static dc field of 0 Oe at various temperatures.

The optimum field to reduce Quantum Tunnelling of Magnetization for **3** was chosen as the one which provides the slowest magnetic relaxation. At 1.8 K the frequency range available was not large enough to allow the precise determination of this optimum field (Figure S24 (top)). Therefore, this determination was performed at 3 K.

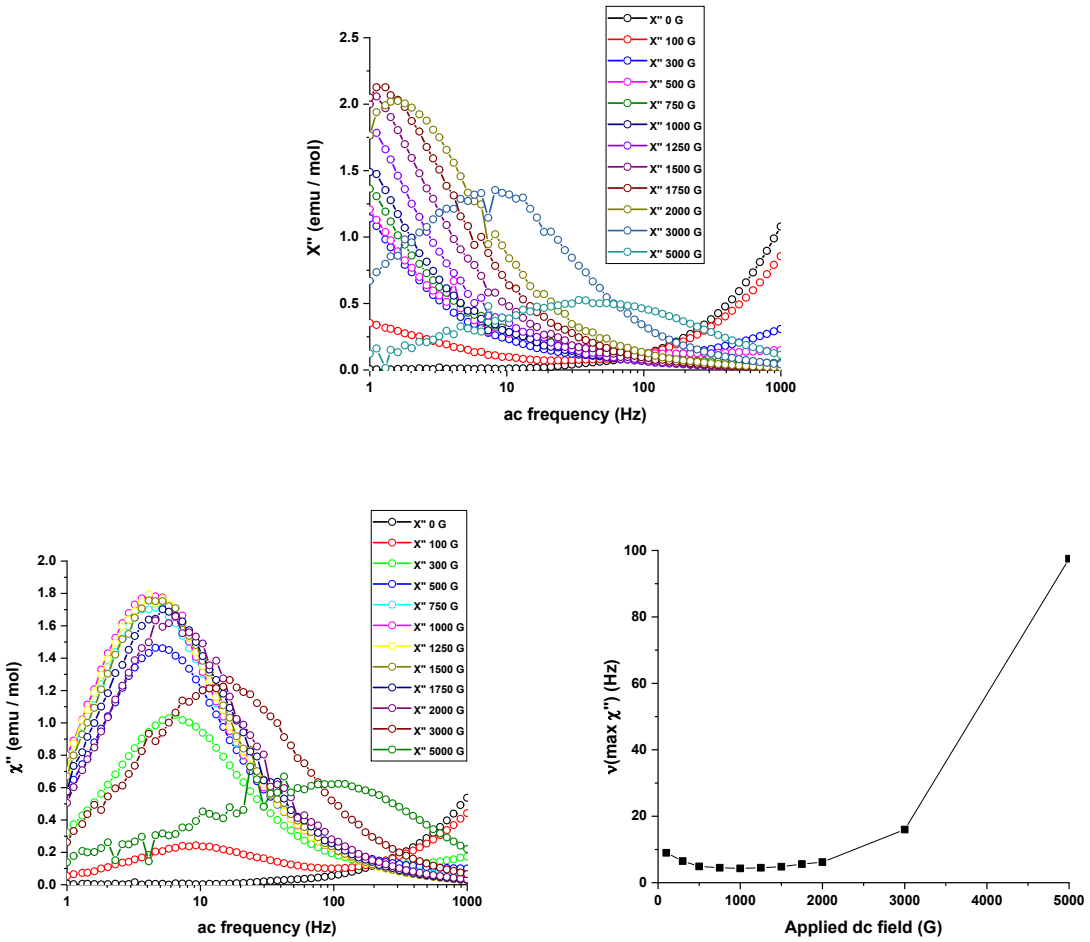

Figure S24. (*top*) Out-of-phase susceptibility curves for complex **3** at 1.8 K with an ac field of 2 Oe and under various applied dc fields. (*Bottom left*) out-of-phase susceptibility curves for complex **3** at 3 K with an ac field of 2 Oe and under various applied dc fields. (*Bottom right*) frequency of the maximum of χ'' as a function of the applied dc field at 3 K.

As can be seen on figure S24, there are (at least) two relaxations modes, one at high frequency in zero field, and another one at low frequencies, which appears when the applied dc field increases.

The low-temperature frequency-dependent ac susceptibility data were further analyzed by using a generalized Debye model to fit the Cole–Cole plot (Figure S25 and Table S14).

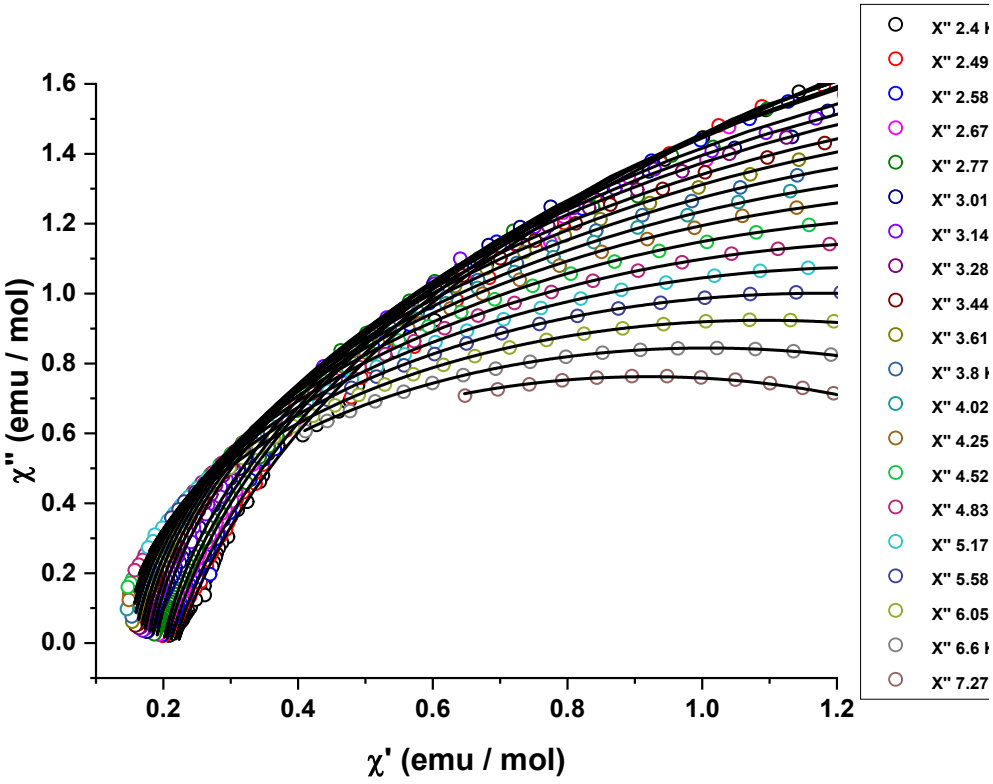

Figure S25. Cole-Cole plots for complex **3** under a static dc field of 1000 Oe at various temperatures.

The parameters obtained from the fits are collected in table S14 below:

Table S14. Parameters of the extended Debye model used to fit the Cole–Cole plots for **3** at various temperatures and under an applied dc field of 1000 Oe.

T (K)	χ_0 (emu / mol)	χ_∞ (emu / mol)	τ (s)	α
1.80	12.2220	0.2627	1.90319	0.2321
1.85	8.9578	0.2615	1.04479	0.2147
1.90	8.8432	0.2541	0.93656	0.2144
1.95	7.4482	0.2470	0.62194	0.1834
2.00	7.5388	0.2448	0.57998	0.1826
2.06	7.1515	0.2416	0.48103	0.1714
2.12	6.5969	0.2377	0.3779	0.1557
2.18	6.3283	0.2328	0.31329	0.1462
2.25	5.9303	0.2281	0.24791	0.1313
2.32	5.6339	0.2245	0.19943	0.1196
2.40	5.3482	0.2213	0.15899	0.1063
2.49	5.0972	0.2164	0.12616	0.09563
2.58	4.8743	0.2101	0.09988	0.08541
2.67	4.6785	0.2042	0.07874	0.08015
2.77	4.4715	0.2000	0.06114	0.06979

3.01	4.0908	0.1886	0.03628	0.05728
3.14	3.9119	0.1821	0.02763	0.05282
3.28	3.7366	0.1770	0.02088	0.04741
3.44	3.5691	0.1696	0.01564	0.04647
3.61	3.4025	0.1641	0.01156	0.04295
3.80	3.2375	0.1573	0.00848	0.04209
4.02	3.0679	0.1509	0.0061	0.04075
4.25	2.8968	0.1460	0.00433	0.03728
4.52	2.7287	0.1416	0.00304	0.03519
4.83	2.5583	0.1377	0.0021	0.03273
5.17	2.3903	0.1358	0.00142	0.02959
5.58	2.2188	0.1348	9.439*10-4	0.02555
6.05	2.0492	0.1339	6.129*10-4	0.02306
6.60	1.8786	0.1350	3.864*10-4	0.0204
7.27	1.7087	0.1317	2.334*10-4	0.02153
8.09	1.5383	0.1159	1.313*10-4	0.02459

The values of α and τ are consistent with those usually encountered for other SMMs (actually, it is better to limit oneself to 2.4-8 K for which a clear maximum of the χ" = f(ν) is visible) The best fits of the Cole–Cole plots in the temperature range 2.4-8.09 K lead to very small α values which indicates a narrow distribution of the relaxation times.

For Complex 4

From the plot of the frequency of the maximum of χ" as a function of temperature, we can extract the various relaxation regimes under a 0 dc field (Table S14).

Table S15. Relaxation times for 4 at various temperatures and under an applied dc field of 0 Oe.

T (K)	τ ($\times 10^{-3}$ s)
1.80	22.93
1.85	22.01
1.90	21.71
1.95	21.25
2.00	20.97
2.06	19.84
2.12	19.46
2.18	18.66
2.25	16.68
2.32	13.11
2.40	8.20
2.49	3.91
2.58	0.231

Supporting information corresponding to the Computational section

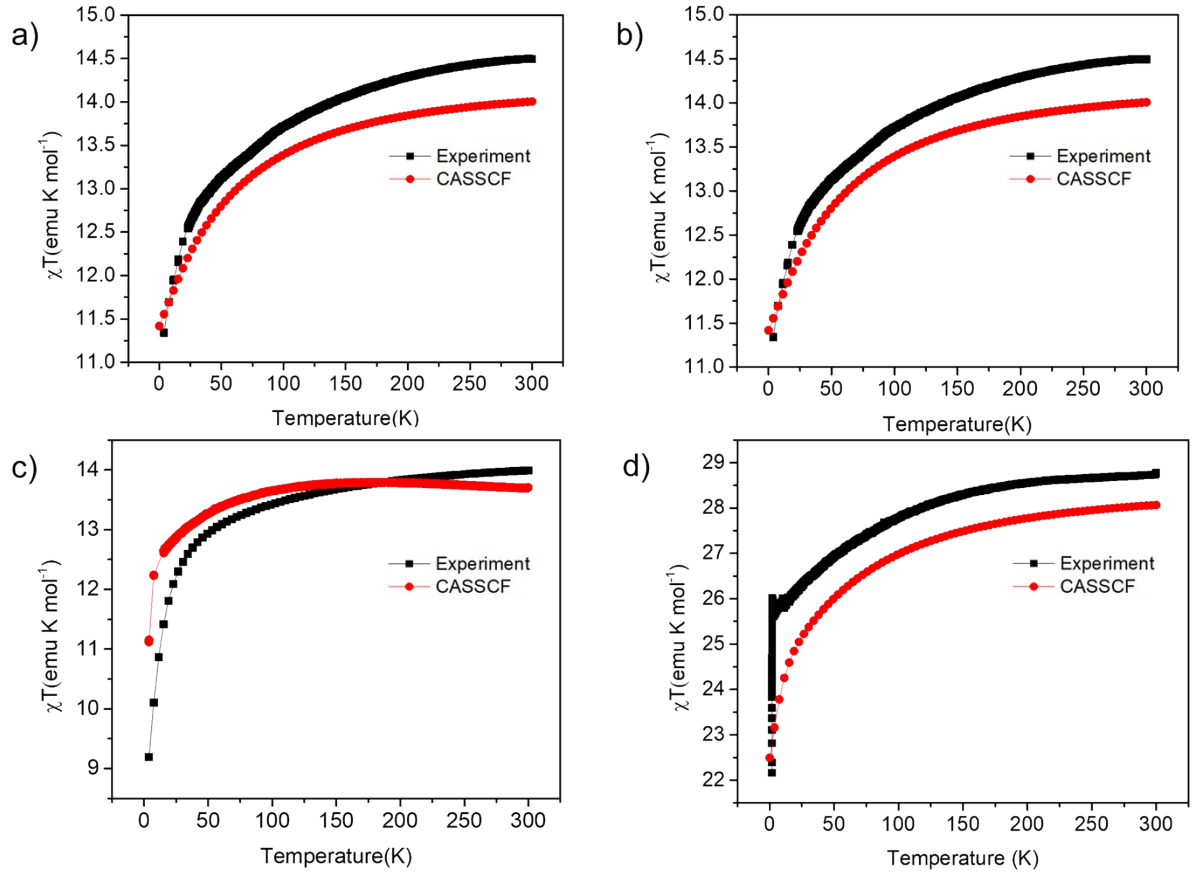

Figure S26. CASSCF computed χT versus T plots for complexes a) **1**, b) **2**, c) **3** and d) **4.** (For complex **4**, the CASSCF computed χT is the sum of the χT values of individual single Dy(III) ions).

Table S16. SINGLE_ANISO computed g-values of the first excited KD, Ucal values tunneling coefficients for complexes **1**–**4**.

Complexes	g_x	g_y	g_z	U_{cal}/cm^{-1}	k_{QTM}
1	0.9410	1.7807	17.5915	77.3	7.73E-01
2	0.1385	0.2350	19.0386	51.5	7.01E-02
3	1.2604	2.1540	10.6922	29.3	5.73E-01
4(Dy@1)	0.0456	0.2451	19.1090	19.2	0.54E-01
4(Dy@2)	0.0457	0.2450	19.1044	19.2	0.54E-01

Table S17. Average axial and equatorial bond lengths of the hydrogen-optimised structures of complexes **1** to **4.**

	Avg. axial bond lengths	Avg. equatorial bond lengths	Avg. axial/Avg. equatorial
1	2.364	2.409	0.981
2	2.372	2.398	0.989
3	2.417	2.398	1.008
4	2.389	2.403	0.994

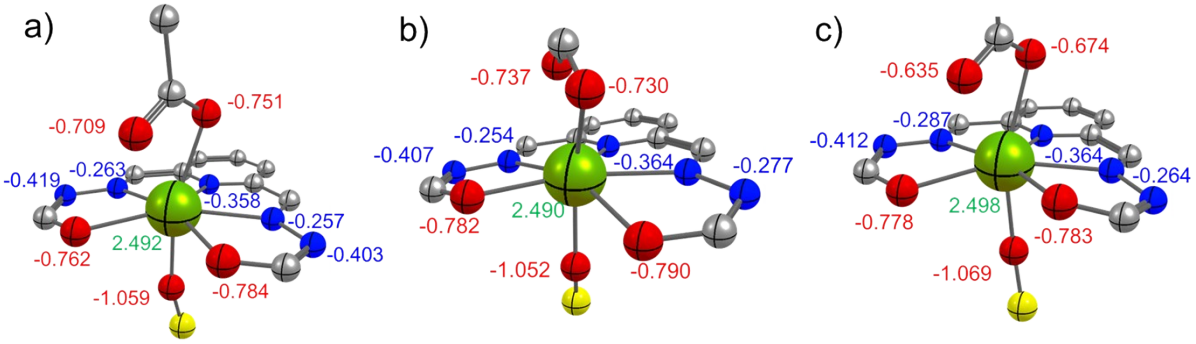

Figure S27. CASSCF computed LoProp charges on first coordination sphere of complex a) **1**, b) **2** and c) **3**. Color code: Green (Dy), red (O), blue (N), yellow (P), grey (C), and white (H).

Table S18. Average axial and equatorial LoProp charges of the hydrogen-optimised structures of complexes **1** to **4.**

	Avg. axial charge	Avg. equatorial charge	Avg. axial/Avg. equatorial
1	-0.839	-0.463	1.812
2	-0.839	-0.466	1.800
3	-0.792	-0.470	1.685
4	-0.834	-0.464	1.797

Table S19. SINGLE_ANISO computed g-tensors, the angle of deviation from ground state g_{zz} orientation and relative energies of eight low lying Kramers doublets for complex **1**.

KDs Energy (cm^{-1})	g_{xx}	g_{yy}	g_{zz}	θ **(° angle)**
0.0	0.0247	0.1323	19.3280	0.0
77.3	0.9410	1.7807	17.5915	123.1
127.4	0.4942	1.8501	15.5875	77.3
204.2	10.2148	7.1521	1.6993	105.5
263.7	2.2631	5.2233	8.6812	99.0
347.9	3.2628	5.3634	12.4348	99.6
391.2	0.6043	2.4534	13.5932	112.8
522.2	0.2686	0.4796	19.1076	82.2

Table S20. SINGLE_ANISO computed g-tensors, the angle of deviation from ground state g_{zz} orientation and relative energies of eight low lying Kramer's doublets for complex **2**.

KDs Energy (cm^{-1})	g_{xx}	g_{yy}	g_{zz}	θ **(° angle)**
0.0	0.0396	0.0987	19.1108	0.0
51.5	0.1385	0.2350	19.0386	39.8
184.9	1.5693	3.9933	11.9934	120.6
223.7	0.5069	4.4031	10.1096	98.8
295.3	1.1848	4.7400	12.3350	92.9
386.2	8.9957	5.5956	1.2168	84.9
453.4	2.3974	3.3495	15.3809	85.6
519.8	0.6028	0.8034	18.2136	105.5

Table S21. SINGLE_ANISO computed g-tensors, the angle of deviation from ground state g_{zz} orientation and relative energies of eight low lying Kramers doublets for complex **3**.

KDs Energy (cm^{-1})	g_{xx}	g_{yy}	g_{zz}	θ **(° angle)**
0.0	0.9045	4.9999	15.4227	0.0
29.3	1.2604	2.1540	10.6922	4.8
86.3	1.7257	2.5601	13.8132	134.8
249.8	1.3605	2.8596	12.1206	13.7
340.0	7.1486	6.2165	2.8538	45.6
405.9	0.0010	2.7413	15.7742	91.7

467.2 545.7	1.8289 0.7797	2.4401 0.8794	15.0049 17.9124	111.8 74.8

Table S22. SINGLE_ANISO computed g-tensors, the angle of deviation from ground state g_{zz} orientation and relative energies of eight low lying Kramers doublets for Dy1 and Dy2 in complex **4** centers respectively.

4 (Dy1)					**4(Dy2)**				
KDs Energy (cm^{-1})	g_{xx}	g_{yy}	g_{zz}	θ (° angle)	KDs Energy (cm^{-1})	g_{xx}	g_{yy}	g_{zz}	θ (° angle)
0.0	0.0269	0.2055	18.9596	0.0	0.0	0.0267	0.2054	18.9553	0.0
19.2	0.0456	0.2451	19.1090	144.3	19.2	0.0457	0.2450	19.1044	144.3
167.0	0.9280	2.1526	13.4089	54.2	167.1	0.9276	2.1507	13.3990	54.2
213.4	0.2445	3.6562	10.5788	70.1	213.5	0.2480	3.6552	10.5751	70.1
289.051	1.5649	4.7243	13.1777	87.0	289.1	1.5678	4.7214	13.1776	87.0
363.1	1.0120	3.6310	9.8583	69.3	363.1	1.0098	3.6276	9.8543	69.4
443.3	2.6744	3.4454	13.5924	104.4	443.4	2.6738	3.4443	13.5914	104.3
529.8	0.5164	0.9615	17.9174	68.3	529.8	0.5159	0.9607	17.9120	68.3

Table S23. SINGLE_ANISO computed crystal field parameters for **1, 2, 3** and **4**. The CF parameters were computed using the following equation, $\hat{H_{CF}} = \Sigma \sum_{k=-q}^{q} B_k^q O_k^q$ and here B_k^q and O_k^q are the crystal field parameters and Steven's operator, respectively.

k	**Q**	B_k^q				
		1	**2**	**3**	**4**	
					Dy1	**Dy2**
2	-2 -1	2.03E+00 7.41E-01	-7.46E-01 -2.35E+00	-2.16E-01 -5.50E-01	-6.70E-01 -3.13E+00	-6.74E-01 -3.14E+00

	0	-1.43E+00	-1.87E+00	-1.66E+00	-1.91E+00	-1.91E+00
	1	-6.99E-01	-2.59E+00	9.61E-02	-3.17E+00	-3.17E+00
	2	9.03E-01	-7.46E-01	3.66E+00	1.01E+00	1.01E+00
4	-4	4.27E-02	2.89E-02	-4.55E-03	3.28E-02	3.26E-02
	-3	2.89E-02	-1.42E-02	-7.03E-02	-1.32E-02	-1.31E-02
	-2	2.31E-03	5.96E-03	7.95E-03	5.06E-03	5.15E-03
	-1	1.20E-02	-9.32E-03	-1.49E-02	-1.32E-03	-1.39E-03
	0	-2.67E-03	-2.68E-03	-2.26E-03	-3.13E-03	-3.13E-03
	1	-1.98E-02	-3.13E-03	-2.04E-03	-4.77E-04	-4.92E-04
	2	7.33E-03	1.76E-04	2.87E-02	-3.39E-03	-3.44E-03
	3	-6.24E-03	2.12E-02	3.66E-02	1.85E-02	1.86E-02
	4	1.32E-02	3.63E-02	-1.65E-02	3.02E-02	3.04E-02
6	-6	1.95E-05	-5.91E-05	-1.17E-04	1.52E-05	1.46E-05
	-5	3.30E-04	-3.19E-04	4.78E-04	-6.38E-04	-6.39E-04
	-4	4.01E-05	-1.32E-05	9.36E-05	-6.28E-05	-6.18E-05
	-3	1.32E-04	1.62E-04	3.03E-04	1.96E-04	1.93E-04
	-2	-4.07E-04	3.30E-04	5.53E-05	2.00E-04	2.01E-04
	-1	-2.38E-04	3.92E-04	5.87E-04	4.23E-04	4.22E-04
	0	-2.27E-05	-8.93E-07	9.74E-07	1.64E-05	1.63E-05
	1	1.83E-04	2.91E-04	2.38E-05	3.08E-04	3.09E-04
	2	2.14E-04	-8.02E-05	-7.66E-05	-1.24E-05	-1.28E-05
	3	-5.79E-06	4.56E-04	-2.30E-05	4.82E-04	4.83E-04
	4	6.99E-05	3.72E-05	1.53E-04	4.41E-05	4.31E-05
	5	7.67E-05	-1.24E-04	1.58E-04	1.03E-04	9.68E-05
	6	-1.22E-04	1.04E-04	-2.04E-04	9.61E-05	9.69E-05

Table S24. SINGLE_ANISO computed wave function decomposition analysis for Dy centre in complex **1**. The major dominating values are kept in bold.

±mJ	*wave function decomposition analysis of complex **1***
KD1	**89.9% |±15/2⟩**+ 8.2 % ±11/2⟩
KD2	**23.1% |±13/2⟩** + 21.8% |±11/2⟩ + 16.4 % |±9/2⟩ + 14.2 % |±7/2⟩ +10.3 % |±5/2⟩ + 8.1 % |±3/2⟩
KD3	**22.9% |±5/2⟩** +22.2% |±7/2⟩ + 16.1% |±9/2⟩ + 12.6 % |±3/2⟩ + 10.4% |±13/2⟩ + 5.3% |±1/2⟩
KD4	**31.4% |±13/2⟩** + 21.6% |±9/2⟩ + 11.2 % |±7/2⟩ **+** 14.1% |±5/2⟩ + 12.1% |±1/2⟩ + 8.8% |±3/2⟩
KD5	**25.7% |±1/2⟩** + 23.1% |±13/2⟩ + 18.3 % |±3/2⟩ +12.6 % |±7/2⟩ +7.4 % |±11/2⟩
KD6	**26.4% |±3/2⟩ +** 26.1 % |±1/2⟩+ 25.6% |±11/2⟩ + 7.9% |±9/2⟩ + 6.1% |±5/2⟩
KD7	**21.6% |±5/2⟩** + 21.5% |±11/2⟩ + 21.4 % |±7/2⟩ + 20.3 % |±9/2⟩ + 8.0% |±13/2⟩
KD8	**24.0% |±3/2⟩**+22.4% |±1/2⟩+ 20.4% |±5/2⟩ + 15.2% |±7/2⟩ + 10.4 |±9/2⟩

Table S25. SINGLE_ANISO computed wave function decomposition analysis for Dy centre in complex **2**. The major dominating values are kept in bold.

±mJ	*wave function decomposition analysis of complex **2***
KD1	**86.1% |±15/2⟩** + 9.0% |±11/2⟩
KD2	**41.3% |±13/2⟩** + 25.4% |±11/2⟩ + 10.7 % |±9/2⟩ + 8.9% |±7/2⟩ +7.3% |±15/2⟩
KD3	**29.9% |±13/2⟩** +21.6% |±9/2⟩+ 16.9%|±1/2⟩+10.9%|±5/2⟩+ 10.1 % |±3/2⟩
KD4	**22.7%|±3/2⟩**+ 18.4% |±9/2⟩ + 13.0 % |±5/2⟩+13.8 % |±13/2⟩ +12.4 % |±11/2⟩**+** 10.4% |±1/2⟩
KD5	**32.0% |±7/2⟩** + 22.7 % |±5/2⟩+ 21.5% |±1/2⟩+10.9%|±3/2⟩ +5.4%|±11/2⟩
KD6	**31.6% |±11/2⟩** + 15.9% |±5/2⟩ + 15.1% |±3/2⟩ + 13.3% |±7/2⟩ + 9.8 % |±9/2⟩ + 17.6% |±1/2⟩
KD7	**25.0% |±1/2⟩** + 18.3% |±3/2⟩ + 16.8% |±9/2⟩ + 16.2 % |±7/2⟩ + 14.5% |±5/2⟩
KD8	**20.8% |±3/2⟩** +18.9% |±5/2⟩ + 19.0% |±9/2⟩ + 17.4% |±1/2⟩ + 13.0 % |±7/2⟩

Table S26. SINGLE_ANISO computed wave function decomposition analysis for Dy centre in complex **3**. The major dominating values are kept in bold.

±mJ	*wave function decomposition analysis of complex 3*
KD1	**56.7% |±15/2⟩**+ 24.6% |±11/2⟩+ 7.4 % |±7/2⟩
KD2	**40.9% |±13/2⟩**+ 29.8% |±9/2⟩ + 8.6 % |±15/2⟩ + 7.2 % |±5/2⟩
KD3	**25.0% |±15/2⟩** + 20.5 % |±7/2⟩ + 12.4% |±3/2⟩ + 11.9 % |±5/2⟩ **+** 10.7 % |±1/2⟩**+ 8.8** % |±11/2⟩
KD4	**31.9% |±13/2⟩ +** 19.2% |±7/2⟩ + 13.7 % |±5/2⟩ + 13.1 % |±11/2⟩+ 6.7 % |±9/2⟩
KD5	**30.0% |±1/2⟩** + 16.5 % |±11/2⟩+15.7% |±5/2⟩ +15.0% |±9/2⟩
KD6	**41.5 % |±3/2⟩** +32.3 % |±1/2⟩ + 12.2 % |±5/2⟩ + 8.4 % |±9/2⟩
KD7	**28.6 % |±7/2⟩** + 22.5 % + |±11/2⟩+19.5% |±9/2⟩+ 15.6 % + |±11/2⟩ +10.0 % + |±1/2⟩
KD8	**27.0% |±5/2⟩**+ 18.7% |±7/2⟩ +18.6 % |±3/2⟩+17.7% |±9/2⟩ +8.5 % |±11/2⟩

Table S27. SINGLE_ANISO computed wave function decomposition analysis for Dy1 centre in complex **4**. The major dominating values are kept in bold.

±m*J*	*wave function decomposition analysis Dy***1**
KD1	**82.8% |±15/2⟩**+ 8.5% |±11/2⟩ + 4.2% |±13/2⟩
KD2	**45.9% |±13/2⟩ +** 24.1% |±11/2⟩ + 11.6% |±15/2⟩+8.6% |±9/2⟩+6.0% |±7/2⟩
KD3	**28.8% |±13/2⟩** + 16.9% |±1/2⟩ + 17.9% |±9/2⟩+ 13.3% |±3/2⟩+ 9.5% |±7/2⟩
KD4	**21.1% |±1/2⟩** + 18.5% |±3/2⟩ + 17.5% |±9/2⟩ + 16.5% |±11/2⟩ + 11.6% |±13/2⟩ + 10.6% |±5/2⟩
KD5	**29.7% |±7/2⟩**+ 24.3% |±5/2⟩ + 19.4% |±1/2⟩ + 16.8% |±3/2⟩
KD6	**24.2% |±11/2⟩** + 19.3% |±7/2⟩ + 19.0% |±5/2⟩ + 16.4% |±3/2⟩+10.5% |±1/2⟩
KD7	**24.4% |±5/2⟩** + 18.7% |±3/2⟩+ 16.7% + |±9/2⟩ + 14.7% |±1/2⟩ + 13.9% |±7/2⟩ + 8.5% |±11/2⟩
KD8	**26.4% |±9/2⟩** + 18.2% |±7/2⟩+ 16.9% |±1/2⟩ + 15.3% |±3/2⟩ + 11.2% |±5/2⟩+10.1% |±11/2⟩

Table S28. SINGLE_ANISO computed wave function decomposition analysis for Dy2 centre, in complex **4**. The major dominating values are kept in bold.

±m*J*	*wave function decomposition analysis Dy***2**
KD1	**82.8% |±15/2⟩**+ 8.5% |±11/2⟩ + 4.2% |±13/2⟩
KD2	**45.9% |±13/2⟩ +** 24.1% |±11/2⟩ + 11.6% |±15/2⟩+8.6% |±9/2⟩+6.0% |±7/2⟩
KD3	**28.8% |±13/2⟩** + 16.9% |±1/2⟩ + 17.9% |±9/2⟩+ 13.3% |±3/2⟩+ 9.5% |±7/2⟩+ 7.7% |±5/2⟩
KD4	**21.1% |±1/2⟩** + 18.6% |±3/2⟩ + 17.6% |±9/2⟩ + 16.5% |±11/2⟩ + 11.6% |±13/2⟩ + 10.5% |±5/2⟩
KD5	**29.8% |±7/2⟩**+ 24.3% |±5/2⟩ + 19.4% |±1/2⟩ + 16.7% |±3/2⟩
KD6	**24.2% |±11/2⟩** + 19.3% |±7/2⟩ + 19.0% |±5/2⟩ + 16.5% |±3/2⟩+10.4% |±1/2⟩
KD7	**24.4% |±5/2⟩** + 18.7% |±3/2⟩+ 16.6% + |±9/2⟩ + 14.7% |±1/2⟩ + 14.0% |±7/2⟩ + 8.5% |±11/2⟩
KD8	**26.4% |±9/2⟩** + 18.2% |±7/2⟩+ 16.9% |±1/2⟩ + 15.3% |±3/2⟩ + 11.2% |±5/2⟩+10.2% |±11/2⟩

POLY_ANISO Simulation Results

Table S29. Exchange and dipolar interaction obtained from the best fit using Lines model for complex **4**.

4	J_{total}	J_{ex}	J_{dipo}	zJ
(Dy)	-0.01	0.009	-0.019	-0.002

Table S30. The energy of the low-lying non-Kramer's exchange doublets along with g_{zz} and tunnelling gap obtained from POLY_ANISO simulation of complex **4**.

Exchange doublets	**Energy/cm^{-1}**	**g_{zz}**	**Δ_{tunnel}**
1	0.000	0.0062	1.4E-05
2	0.164	37.911	1.4E-05
3	19.162	9.788	1.4E-04
4	19.181	9.789	1.1E-04
5	19.298	36.225	1.2E-04
6	19.317	36.224	1.5E-04
7	38.313	0.0061	1.4E-05
8	38.481	38.216	1.4E-05

Table S31. Basis functions used in *ab initio* CASSCF calculations using MOLCAS 8.2 code.

Atoms	**ANO-RCC basis functions**
H	2s
C	3s2p
N, O, F	3s2p
Dy	8s7p5d3f2g1h

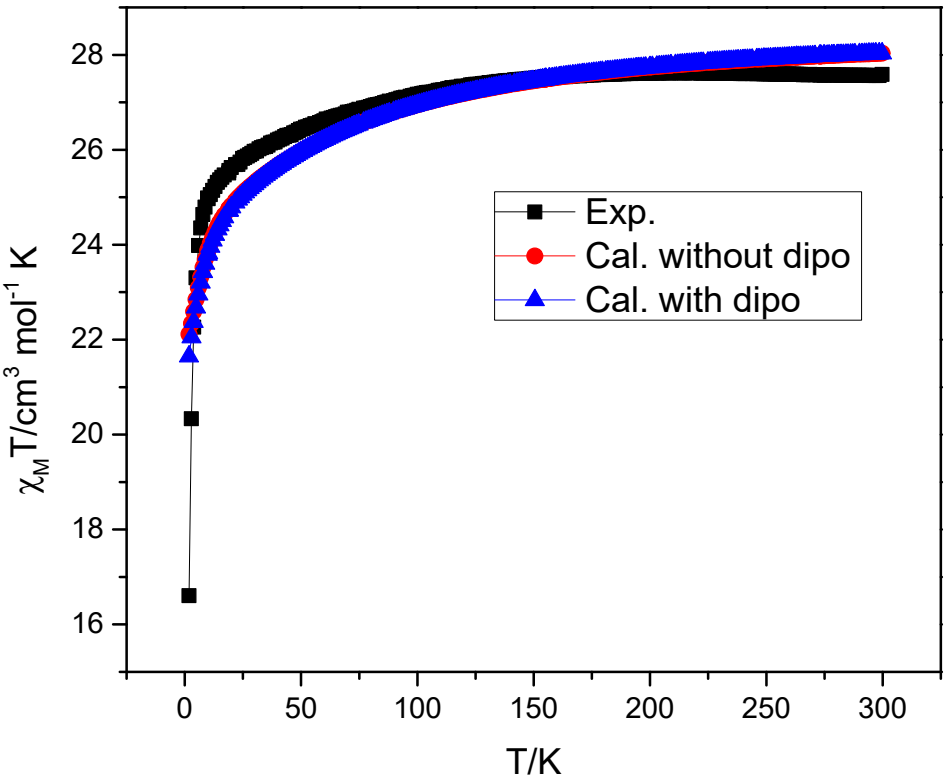

Figure S28. Poly_aniso fit for complex **4**.

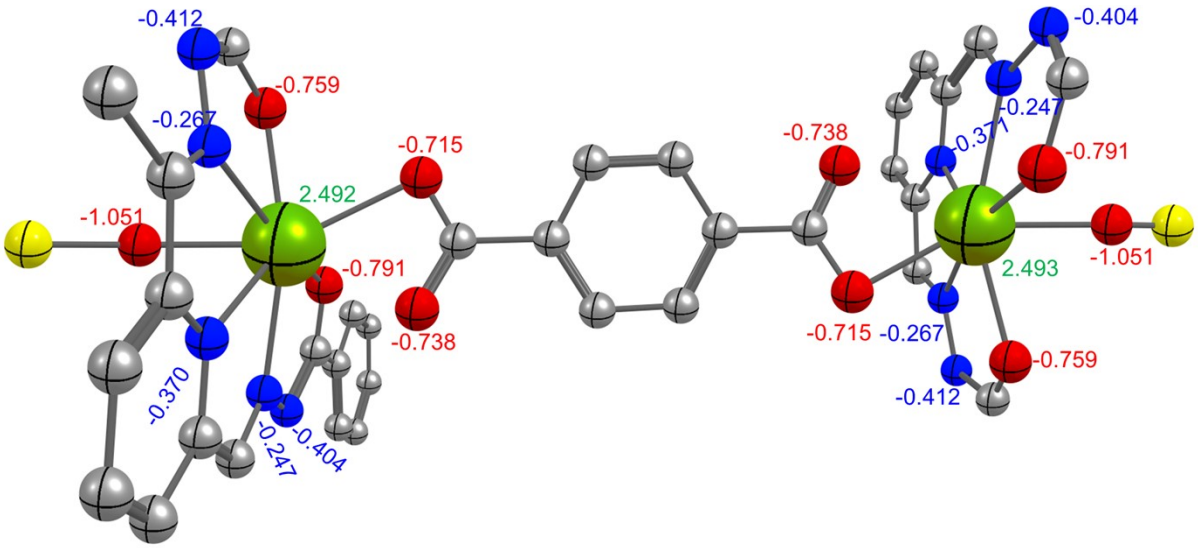

Figure S29. CASSCF computed LoProp charges on the first coordination sphere of complex 4. Color code: Green (Dy), red (O), blue (N), yellow (P), grey (C), and white (H).

Table S32. RASSI-SO computed low-lying 21 spin-free sextet states and the spin-orbit coupled (Kramer doublets) for Dy in complex **1**. All the values are reported here in cm^{-1}.

SPIN-FREE STATES	SPIN-ORBIT STATES	
0.0	0.0	9771.0
13.6	77.3	9800.8
92.4	127.4	9866.4
117.9	204.2	9974.6
212.1	263.7	11065.0
232.6	347.9	11176.0
320.9	391.2	11302.2
447.7	522.2	11802.7
537.4	3060.6	11863.9
642.6	3160.4	11885.0
702.8	3176.4	11909.0
7498.4	3233.6	11930.5
7683.1	3268.5	13570.7
7709.0	3320.9	13644.5
7753.3	3407.8	13697.0
7800.1	5671.9	13715.1
7828.9	5728.9	15006.5
7884.1	5760.1	15047.9
34718.3	5861.2	15082.5
34875.5	5906.2	16036.5
35159.3	5971.5	16050.5
	7881.3	16639.5
	7911.7	38716.6
	7979.0	38797.9
	8076.6	38858.2
	8149.2	38940.2
	9539.0	40115.9
	9597.9	40220.8
	9622.0	40392.6
	9646.8	41223.6
	9687.7	41272.6
	9711.5	

Table S33. RASSI-SO computed low-lying 21 spin-free sextet states and the spin-orbit coupled (Kramer doublets) for Dy in complex **2**. All the values are reported here in cm^{-1}.

SPIN-FREE STATES	SPIN-ORBIT STATES	
0.0	0.0	9800.6
10.6	51.5	9823.0
86.7	184.9	9886.0
101.4	223.7	10002.5
270.5	295.3	11055.7
281.1	386.2	11239.3
335.6	453.4	11314.8
453.3	519.8	11820.9
588.0	3031.5	11891.7
636.2	3191.2	11909.6
736.6	3221.6	11931.9
7526.7	3249.2	11951.7
7668.3	3308.4	13597.5
7727.4	3366.9	13658.6
7767.9	3416.7	13719.3
7837.1	5651.7	13742.2
7841.5	5783.0	15028.1
7904.9	5789.1	15075.4
34643.1	5869.4	15101.0
35007.0	5935.1	16061.0
35145.0	6004.0	16071.3
	7876.7	16662.3
	7949.2	38728.2
	8007.7	38780.6
	8088.7	38854.2
	8184.6	39006.5
	9553.0	40118.0
	9621.6	40280.5
	9641.2	40405.9
	9658.1	41242.3
	9721.3	41301.9
	9735.2	

Table S34. RASSI-SO computed low-lying 21 spin-free sextet states and the spin-orbit coupled (Kramer doublets) for Dy in complex **3**. All the values are reported here in cm^{-1}.

SPIN-FREE STATES	SPIN-ORBIT STATES	
0.0	0.0	9786.2
45.9	29.3	9843.6
55.1	86.3	9876.8
104.2	249.8	10035.5
208.7	340.0	11048.7
220.2	405.9	11220.7
460.6	467.2	11352.9
555.2	545.7	11833.6
596.1	3059.1	11897.5
693.8	3107.4	11916.4
736.8	3181.5	11946.3
7505.2	3285.6	11954.6
7748.6	3327.5	13596.5
7764.3	3382.3	13676.3
7766.6	3457.6	13730.9
7837.5	5686.0	13746.2
7867.4	5727.5	15034.3
7925.1	5758.3	15080.7
34734.6	5903.5	15114.0
34830.7	5934.5	16066.7
35307.1	6039.7	16083.1
	7903.8	16671.4
	7934.8	38698.2
	7963.3	38812.9
	8106.1	38904.2
	8215.3	38979.9
	9533.1	40107.0
	9631.0	40231.9
	9657.2	40502.3
	9678.3	41266.3
	9713.1	41329.7
	9739.2	

Table S35. RASSI-SO computed low-lying 21 spin-free sextet states and the spin-orbit coupled (Kramer doublets) for Dy@1 in complex **4**. All the values are reported here in cm^{-1}.

4(Dy1)		
SPIN-FREE STATES	**SPIN-ORBIT STATES**	
0.0	0.0	9821.5
16.7	19.2	9869.9
53.9	167.1	9993.5
58.7	213.5	11036.5
250.9	289.1	11228.1
266.5	363.1	11323.6
324.5	443.4	11808.2
419.0	529.9	11881.8
558.3	3009.3	11900.7
644.0	3156.2	11920.3
729.0	3222.2	11938.2
7519.9	3247.4	13590.7
7652.5	3301.4	13647.1
7702.9	3358.3	13708.3
7749.5	3414.0	13731.6
7811.5	5633.0	15018.4
7832.7	5757.2	15070.0
7895.0	5798.9	15088.1
34606.6	5853.8	16051.5
35012.3	5929.6	16062.7
35142.0	5998.3	16654.0
	7860.5	38712.0
	7938.9	38763.8
	8002.9	38843.8
	8078.2	39013.3
	8179.4	40104.7
	9543.9	40280.9
	9610.7	40409.4
	9630.4	41237.9
	9650.1	41302.1
	9708.5	
	9727.1	
	9785.1	

Table S36. RASSI-SO computed low-lying 21 spin-free sextet states and the spin-orbit coupled (Kramer doublets) for Dy@2 in complex **4**. All the values are reported here in cm^{-1}.

4(Dy2)		
SPIN-FREE STATES	**SPIN-ORBIT STATES**	
0.0	0.0	9821.5
16.7	19.2	9869.8
53.8	167.1	9993.4
58.6	213.5	11036.5
250.9	289.1	11228.1
266.4	363.1	11323.5
324.5	443.4	11808.2
419.1	529.8	11881.8
558.3	3009.2	11900.7
643.9	3156.1	11920.3
729.0	3222.1	11938.1
7519.9	3247.3	13590.7
7652.5	3301.3	13647.0
7702.8	3358.3	13708.3
7749.4	3413.9	13731.5
7811.5	5632.9	15018.3
7832.7	5757.2	15070.0
7894.9	5798.9	15088.1
34606.5	5853.7	16051.4
35012.3	5929.6	16062.7
35142.0	5998.2	16653.9
	7860.4	38712.0
	7938.9	38763.8
	8002.9	38843.8
	8078.2	39013.2
	8179.4	40104.6
	9543.8	40280.8
	9610.7	40409.4
	9630.3	41237.8
	9650.0	41302.1
	9708.5	
	9727.1	
	9785.1	

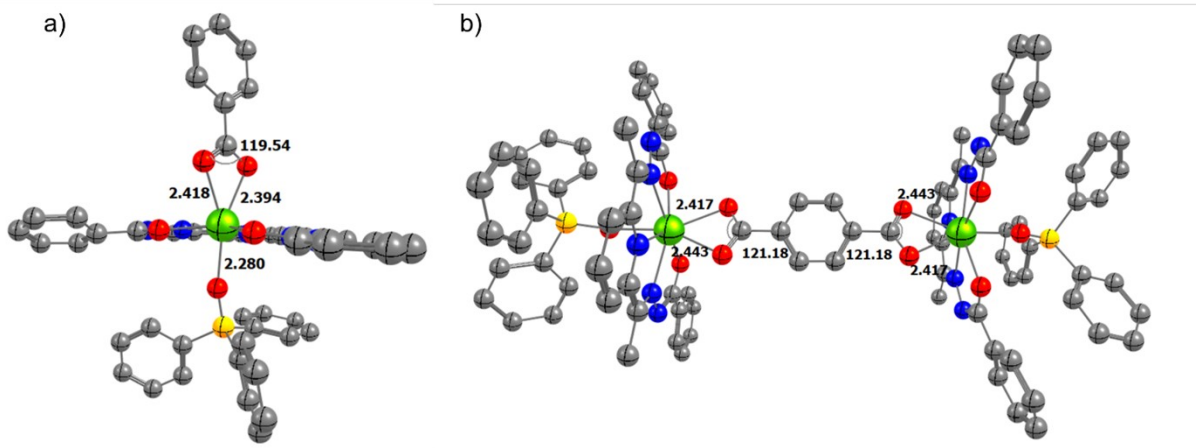

Figure S30. Comparison of the bite/cone angle and DyO1/DyO2 bond distances in complex a) **1** and b) **4**.

Table S37. Hydrogen optimized cartesian coordinates of complexes **1**, **2**, **3**, **4**.

Complex **1**

Dy	0.000000000000	0.000000000000	0.000000000000
P	0.000000000000	0.000000000000	3.742071000000
O	-2.290729000000	-0.181355000000	0.112150000000
O	0.250207000000	2.277665000000	0.115401000000
O	-0.235482000000	0.048862000000	2.266918000000
O	-0.837481000000	0.532953000000	-2.204969000000
O	1.110808000000	-0.419784000000	-2.079100000000
N	-2.250467000000	-2.496074000000	0.283732000000
N	-0.872458000000	-2.303301000000	0.294329000000
N	1.679398000000	-1.767236000000	0.511484000000
N	2.296628000000	0.803140000000	0.469078000000
N	2.532691000000	2.165484000000	0.475999000000
C	-2.860931000000	-1.323222000000	0.203956000000
C	-0.124545000000	-3.342519000000	0.483648000000
C	1.323408000000	-3.064627000000	0.569278000000
C	2.279165000000	-4.080598000000	0.718295000000
C	3.604300000000	-3.742511000000	0.802982000000
C	3.966471000000	-2.416323000000	0.755666000000
C	2.984992000000	-1.433679000000	0.620613000000
C	3.303844000000	-0.001155000000	0.584400000000
C	1.400459000000	2.817076000000	0.289565000000
C	-0.645053000000	-4.738084000000	0.619804000000
C	4.723729000000	0.463606000000	0.702772000000
C	-4.345715000000	-1.343904000000	0.240149000000
C	-4.964420000000	-2.538691000000	0.669712000000
C	-6.351243000000	-2.613332000000	0.620527000000
C	-7.044466000000	-1.577801000000	0.040684000000

C	-6.460533000000	-0.408566000000	-0.413113000000
C	-5.075327000000	-0.365445000000	-0.406228000000
C	1.482824000000	4.302548000000	0.270872000000
C	0.329360000000	5.053834000000	0.146584000000
C	0.370131000000	6.445111000000	0.107370000000
C	1.576171000000	7.096063000000	0.174412000000
C	2.733316000000	6.358422000000	0.311303000000
C	2.702970000000	4.977218000000	0.365215000000
C	-1.333699000000	-0.884121000000	4.560445000000
C	-1.257915000000	-1.232183000000	5.895452000000
C	-2.346735000000	-1.810411000000	6.525345000000
C	-3.494484000000	-2.055713000000	5.814520000000
C	-3.572829000000	-1.737978000000	4.481497000000
C	-2.495189000000	-1.138425000000	3.847930000000
C	-0.001895000000	1.663433000000	4.411262000000
C	0.178755000000	1.946600000000	5.761126000000
C	0.044465000000	3.248075000000	6.213684000000
C	-0.270937000000	4.260791000000	5.331927000000
C	-0.420139000000	3.999078000000	3.992457000000
C	-0.287202000000	2.699404000000	3.526137000000
C	1.547419000000	-0.812276000000	4.139681000000
C	2.703904000000	-0.077726000000	4.377177000000
C	3.921514000000	-0.725739000000	4.493498000000
C	3.990518000000	-2.103964000000	4.373396000000
C	2.850778000000	-2.841079000000	4.134680000000
C	1.632858000000	-2.199610000000	4.017616000000
C	0.155379000000	0.000000000000	-2.772165000000
C	0.157532000000	-0.152699000000	-4.246038000000
C	1.261571000000	-0.702157000000	-4.883574000000
C	1.247631000000	-0.870344000000	-6.253911000000
C	0.133796000000	-0.537833000000	-6.977890000000
C	-0.964994000000	0.009315000000	-6.360560000000
C	-0.948878000000	0.215797000000	-4.991422000000
H	1.958199000000	-5.131485000000	0.756515000000
H	4.374489000000	-4.523685000000	0.909127000000
H	5.023479000000	-2.124355000000	0.830639000000
H	-1.748372000000	-4.723778000000	0.515028000000
H	-0.383911000000	-5.181097000000	1.610506000000
H	-0.218354000000	-5.408289000000	-0.163161000000
H	4.744732000000	1.571362000000	0.679218000000
H	5.350279000000	0.075121000000	-0.134247000000
H	5.185311000000	0.112505000000	1.655949000000
H	-4.338917000000	-3.344009000000	1.080587000000
H	-6.883239000000	-3.512865000000	0.971303000000
H	-8.146662000000	-1.661056000000	-0.013924000000
H	-7.062078000000	0.393886000000	-0.866804000000
H	-4.522590000000	0.497918000000	-0.815248000000
H	-0.629037000000	4.514862000000	0.064143000000
H	-0.569801000000	7.012152000000	0.001929000000
H	1.623068000000	8.196995000000	0.127448000000

H	3.705950000000	6.876456000000	0.372840000000
H	3.627938000000	4.389866000000	0.468153000000
H	-0.327714000000	-1.061901000000	6.465695000000
H	-2.281821000000	-2.078370000000	7.592530000000
H	-4.359970000000	-2.518974000000	6.317600000000
H	-4.488541000000	-1.943614000000	3.903811000000
H	-2.549875000000	-0.853354000000	2.783665000000
H	0.422382000000	1.144028000000	6.477968000000
H	0.182081000000	3.468575000000	7.284981000000
H	-0.386490000000	5.291622000000	5.706857000000
H	-0.642147000000	4.807675000000	3.277954000000
H	-0.411882000000	2.475162000000	2.451354000000
H	2.651420000000	1.021861000000	4.451976000000
H	4.836029000000	-0.139582000000	4.679296000000
H	4.965292000000	-2.611484000000	4.462543000000
H	2.904889000000	-3.935748000000	4.027395000000
H	0.719183000000	-2.783869000000	3.809698000000
H	2.132988000000	-0.987364000000	-4.272364000000
H	2.129006000000	-1.297212000000	-6.762232000000
H	0.123338000000	-0.698484000000	-8.069998000000
H	-1.855616000000	0.285919000000	-6.948951000000
H	-1.811116000000	0.654398000000	-4.463503000000

Complex **2**

Dy	0.000000000000	0.000000000000	0.000000000000
P	0.000000000000	0.000000000000	3.748893000000
O	-2.319612000000	-0.181249000000	0.113395000000
O	-0.263025000000	-0.191613000000	2.284209000000
O	0.615840000000	-2.203158000000	0.029668000000
O	1.248505000000	0.439950000000	-2.024331000000
O	-0.777841000000	-0.305508000000	-2.239573000000
N	-2.637082000000	2.096263000000	-0.134596000000
N	-1.236909000000	2.111025000000	0.072516000000
N	1.330386000000	2.006202000000	0.517190000000
N	2.346174000000	-0.410079000000	0.633207000000
N	2.795775000000	-1.723569000000	0.707559000000
C	-3.036096000000	0.890031000000	-0.078779000000
C	-0.677164000000	3.270135000000	0.149646000000
C	0.779807000000	3.252939000000	0.430208000000
C	1.540713000000	4.409789000000	0.599197000000
C	2.865880000000	4.285094000000	0.870268000000
C	3.395401000000	2.999926000000	0.991606000000
C	2.641496000000	1.908266000000	0.798651000000
C	3.170104000000	0.556666000000	0.857902000000
C	1.806500000000	-2.556923000000	0.365118000000
C	4.653451000000	0.268503000000	1.162776000000
C	-1.398072000000	4.596076000000	0.064949000000
C	-4.508484000000	0.660250000000	-0.259480000000
C	-6.430531000000	-0.770817000000	-0.290728000000

C	-5.076187000000	-0.552989000000	-0.145368000000
C	2.111262000000	-4.000816000000	0.496345000000
C	1.206888000000	-4.914886000000	-0.027980000000
C	1.407370000000	-6.269184000000	0.094823000000
C	2.499515000000	-6.741104000000	0.818235000000
C	3.429159000000	-5.825558000000	1.334348000000
C	3.213999000000	-4.450980000000	1.147494000000
C	0.332230000000	0.000000000000	-2.748331000000
C	0.490032000000	-0.129712000000	-4.254991000000
C	1.726217000000	0.500649000000	-4.724578000000
C	-0.778930000000	0.481069000000	-4.879221000000
C	0.470052000000	-1.641869000000	-4.545185000000
C	0.610912000000	-1.486137000000	4.497702000000
C	0.729222000000	-2.636885000000	3.662787000000
C	1.264155000000	-3.822426000000	4.179660000000
C	1.567621000000	-3.900185000000	5.546649000000
C	1.441318000000	-2.789854000000	6.370595000000
C	0.971412000000	-1.582123000000	5.841035000000
C	1.181124000000	1.277525000000	4.049170000000
C	2.548813000000	1.028327000000	4.282520000000
C	3.455929000000	1.994128000000	4.405089000000
C	3.023228000000	3.357442000000	4.304075000000
C	1.675095000000	3.578929000000	4.033419000000
C	0.809295000000	2.593533000000	3.922753000000
C	-1.550803000000	0.449911000000	4.541810000000
C	-1.738258000000	0.520922000000	5.918702000000
C	-2.992936000000	0.797374000000	6.450754000000
C	-4.046128000000	0.987288000000	5.620236000000
C	-3.904442000000	0.933446000000	4.242628000000
C	-2.663152000000	0.659493000000	3.700843000000
C	-7.206126000000	0.292495000000	-0.671185000000
C	-5.275476000000	1.718529000000	-0.817731000000
C	-6.662367000000	1.524006000000	-1.046114000000
H	1.065164000000	5.396408000000	0.502358000000
H	3.511471000000	5.165771000000	1.010876000000
H	4.464681000000	2.885838000000	1.223992000000
H	4.778122000000	-0.828679000000	1.249737000000
H	4.978185000000	0.763216000000	2.107070000000
H	5.307433000000	0.642834000000	0.340160000000
H	-2.464137000000	4.414364000000	-0.176122000000
H	-0.950176000000	5.248220000000	-0.719818000000
H	-1.338707000000	5.146129000000	1.034004000000
H	-6.869334000000	-1.762477000000	-0.100963000000
H	-4.414496000000	-1.386348000000	0.152092000000
H	0.323428000000	-4.517093000000	-0.553368000000
H	0.684246000000	-6.978186000000	-0.340994000000
H	2.653879000000	-7.824492000000	0.956137000000
H	4.314739000000	-6.177608000000	1.887871000000
H	3.932019000000	-3.719530000000	1.550148000000
H	1.748778000000	1.592941000000	-4.500202000000

H	1.848051000000	0.383306000000	-5.828477000000
H	2.625309000000	0.060598000000	-4.235837000000
H	-1.687257000000	-0.001901000000	-4.461185000000
H	-0.770496000000	0.345677000000	-5.987147000000
H	-0.844961000000	1.575240000000	-4.668904000000
H	1.340203000000	-2.154770000000	-4.070979000000
H	0.520611000000	-1.827461000000	-5.644676000000
H	-0.460659000000	-2.104813000000	-4.149615000000
H	0.433743000000	-2.558636000000	2.602911000000
H	1.397846000000	-4.694069000000	3.520147000000
H	1.950004000000	-4.847640000000	5.962429000000
H	1.709221000000	-2.851432000000	7.437632000000
H	0.926115000000	-0.695786000000	6.496899000000
H	2.868634000000	-0.027580000000	4.354256000000
H	4.516472000000	1.765376000000	4.594448000000
H	3.735388000000	4.190024000000	4.407317000000
H	1.331092000000	4.621384000000	3.922485000000
H	-0.252682000000	2.822848000000	3.714432000000
H	-0.891411000000	0.365912000000	6.607446000000
H	-3.118476000000	0.846222000000	7.544446000000
H	-5.043859000000	1.194783000000	6.044664000000
H	-4.769573000000	1.087457000000	3.578741000000
H	-2.525321000000	0.559032000000	2.609452000000
H	-8.297548000000	0.149595000000	-0.780329000000
H	-4.783970000000	2.677281000000	-1.039946000000
H	-7.292969000000	2.330625000000	-1.451499000000

Complex **3**

Dy	0.000000000000	0.000000000000	0.000000000000
P	0.000000000000	0.000000000000	3.776797000000
F	-0.675504000000	-0.508935000000	-4.887834000000
F	0.621380000000	1.195732000000	-4.836003000000
F	1.431185000000	-0.772633000000	-4.696912000000
O	2.150317000000	0.718562000000	0.199320000000
O	-0.074971000000	-0.018781000000	2.280174000000
O	-1.158220000000	1.979299000000	0.176171000000
O	0.128525000000	-1.072901000000	-2.210441000000
O	0.371377000000	1.118539000000	-2.218410000000
N	2.938690000000	-1.367868000000	0.842304000000
N	1.636622000000	-1.760128000000	0.556182000000
N	-0.916991000000	-2.302904000000	0.245254000000
N	-2.447612000000	-0.199696000000	-0.073980000000
N	-3.212744000000	0.953803000000	-0.167506000000
C	3.066600000000	-0.068674000000	0.635383000000
C	1.336946000000	-3.010457000000	0.686130000000
C	-0.077734000000	-3.343512000000	0.435340000000
C	-0.554734000000	-4.663598000000	0.435951000000
C	-1.899604000000	-4.888388000000	0.261995000000
C	-2.762355000000	-3.818460000000	0.103741000000

C	-2.230467000000	-2.530889000000	0.083808000000
C	-3.083616000000	-1.332762000000	-0.072445000000
C	-2.423861000000	2.014000000000	-0.031747000000
C	-4.563458000000	-1.447816000000	-0.186346000000
C	2.292106000000	-4.078315000000	1.117794000000
C	4.399175000000	0.524961000000	0.931235000000
C	5.443545000000	-0.234898000000	1.442476000000
C	6.651173000000	0.370068000000	1.755682000000
C	6.847827000000	1.718873000000	1.541796000000
C	5.825592000000	2.460939000000	1.029291000000
C	4.606830000000	1.875503000000	0.728423000000
C	-3.093557000000	3.342052000000	-0.141968000000
C	-4.462531000000	3.442186000000	-0.377560000000
C	-5.051988000000	4.689910000000	-0.499357000000
C	-4.306269000000	5.842296000000	-0.379423000000
C	-2.949657000000	5.743265000000	-0.140128000000
C	-2.342163000000	4.503493000000	-0.028173000000
C	0.296009000000	0.000000000000	-2.772696000000
C	0.407997000000	-0.018307000000	-4.311222000000
C	-1.562949000000	0.578987000000	4.452138000000
C	-2.459811000000	1.210778000000	3.604916000000
C	-3.686186000000	1.644972000000	4.088651000000
C	-4.023212000000	1.441797000000	5.406656000000
C	-3.150668000000	0.806375000000	6.247815000000
C	-1.901798000000	0.369174000000	5.788675000000
C	-0.336656000000	-2.741599000000	3.826619000000
C	-0.159246000000	-4.019950000000	4.332683000000
C	0.605719000000	-4.229922000000	5.449244000000
C	1.223895000000	-3.151966000000	6.059189000000
C	1.072894000000	-1.874767000000	5.562532000000
C	0.279413000000	-1.648351000000	4.440786000000
C	1.333188000000	1.037671000000	4.388675000000
C	1.097026000000	2.178500000000	5.168964000000
C	2.173404000000	2.958354000000	5.580711000000
C	3.462721000000	2.624758000000	5.222365000000
C	3.698472000000	1.503985000000	4.424973000000
C	2.642248000000	0.717263000000	4.011753000000
H	0.144526000000	-5.500889000000	0.570422000000
H	-2.292399000000	-5.918216000000	0.256747000000
H	-3.842480000000	-3.977478000000	-0.020030000000
H	-5.013307000000	-1.891559000000	0.733990000000
H	-4.855905000000	-2.100404000000	-1.042032000000
H	-4.997481000000	-0.440059000000	-0.340067000000
H	2.437822000000	-4.844083000000	0.319921000000
H	1.916780000000	-4.604589000000	2.026485000000
H	3.275475000000	-3.620630000000	1.345545000000
H	5.292269000000	-1.313606000000	1.603090000000
H	7.469793000000	-0.245678000000	2.166179000000
H	7.817793000000	2.183924000000	1.783976000000
H	5.958688000000	3.540832000000	0.847870000000

H	3.773833000000	2.472017000000	0.323429000000
H	-5.055327000000	2.520454000000	-0.477633000000
H	-6.135782000000	4.756153000000	-0.696426000000
H	-4.785267000000	6.830460000000	-0.477791000000
H	-2.337539000000	6.656262000000	-0.048360000000
H	-1.258174000000	4.408783000000	0.143967000000
H	-2.185047000000	1.367677000000	2.548359000000
H	-4.383218000000	2.148576000000	3.399544000000
H	-5.000979000000	1.784183000000	5.783977000000
H	-3.421761000000	0.633269000000	7.302638000000
H	-1.210805000000	-0.151183000000	6.473701000000
H	-0.958603000000	-2.580138000000	2.930046000000
H	-0.650678000000	-4.865935000000	3.823988000000
H	0.738386000000	-5.245457000000	5.855984000000
H	1.851981000000	-3.313196000000	6.950958000000
H	1.584320000000	-1.029686000000	6.053678000000
H	0.067598000000	2.451526000000	5.454385000000
H	1.985258000000	3.853638000000	6.196041000000
H	4.308363000000	3.251056000000	5.549924000000
H	4.722011000000	1.250183000000	4.104817000000
H	2.833065000000	-0.163445000000	3.372564000000

Complex **4**

Dy	0.000000000000	0.000000000000	0.000000000000
Dy	-6.013492000000	-6.429318000000	-7.180674000000
P	2.261936000000	1.787656000000	2.377678000000
P	-8.275428000000	-8.216974000000	-9.558352000000
O	-1.433261000000	1.756552000000	-0.314210000000
O	-0.800485000000	-0.833009000000	1.996707000000
O	1.133703000000	1.327604000000	1.510064000000
O	-0.523519000000	-0.834193000000	-2.235317000000
O	-1.638636000000	-1.687634000000	-0.556376000000
O	-5.489973000000	-5.595125000000	-4.945357000000
O	-4.374856000000	-4.741684000000	-6.624297000000
O	-4.580231000000	-8.185870000000	-6.866464000000
O	-5.213007000000	-5.596309000000	-9.177381000000
O	-7.147195000000	-7.756922000000	-8.690738000000
N	0.040792000000	2.871691000000	-1.733626000000
N	0.825285000000	1.745923000000	-1.532705000000
N	2.237735000000	-0.397148000000	-1.009516000000
N	1.310625000000	-1.853880000000	0.971121000000
N	0.865991000000	-2.449229000000	2.137429000000
N	-6.054284000000	-9.301009000000	-5.447048000000
N	-6.838777000000	-8.175241000000	-5.647969000000
N	-8.251227000000	-6.032170000000	-6.171158000000
N	-7.324117000000	-4.575438000000	-8.151795000000
N	-6.879483000000	-3.980089000000	-9.318103000000
C	-1.093288000000	2.750798000000	-1.065298000000
C	1.909382000000	1.656374000000	-2.220760000000

C	2.714990000000	0.445975000000	-1.954032000000
C	3.912756000000	0.166023000000	-2.616837000000
C	4.591991000000	-0.994897000000	-2.325137000000
C	4.104463000000	-1.856914000000	-1.359884000000
C	2.920643000000	-1.518147000000	-0.693488000000
C	2.390754000000	-2.322102000000	0.429111000000
C	-0.198903000000	-1.795764000000	2.584340000000
C	3.135955000000	-3.523862000000	0.922910000000
C	2.361179000000	2.681202000000	-3.218198000000
C	-2.043977000000	3.881507000000	-1.223036000000
C	-1.829069000000	4.879836000000	-2.166961000000
C	-2.726654000000	5.924882000000	-2.292494000000
C	-3.862215000000	5.972754000000	-1.509876000000
C	-4.101313000000	4.978211000000	-0.583845000000
C	-3.187059000000	3.936759000000	-0.436845000000
C	-0.709123000000	-2.202974000000	3.926955000000
C	0.003188000000	-3.060908000000	4.751603000000
C	-0.449413000000	-3.336181000000	6.024527000000
C	-1.629943000000	-2.782978000000	6.488885000000
C	-2.359409000000	-1.956179000000	5.666011000000
C	-1.909804000000	-1.660726000000	4.398453000000
C	-1.413502000000	-1.601290000000	-1.788501000000
C	-2.225267000000	-2.441676000000	-2.740396000000
C	-2.973936000000	-3.508404000000	-2.236677000000
C	-3.754913000000	-4.276206000000	-3.081252000000
C	1.881473000000	1.576964000000	4.125602000000
C	0.749648000000	0.853023000000	4.461064000000
C	0.448641000000	0.597149000000	5.798450000000
C	1.256112000000	1.097288000000	6.802155000000
C	2.332603000000	1.868401000000	6.464881000000
C	2.676513000000	2.089429000000	5.145396000000
C	3.779262000000	0.877221000000	2.054013000000
C	4.091192000000	-0.248493000000	2.805086000000
C	5.236579000000	-0.978553000000	2.506989000000
C	6.058643000000	-0.608735000000	1.461387000000
C	5.748563000000	0.514116000000	0.699585000000
C	4.611919000000	1.252927000000	0.992322000000
C	2.626987000000	3.522930000000	2.055519000000
C	3.785418000000	4.146667000000	2.526546000000
C	4.016256000000	5.480866000000	2.256833000000
C	3.097519000000	6.199530000000	1.494640000000
C	1.959602000000	5.579366000000	1.012895000000
C	1.712968000000	4.242726000000	1.291541000000
C	-4.599990000000	-4.828028000000	-5.392173000000
C	-3.788225000000	-3.987642000000	-4.440278000000
C	-3.039556000000	-2.920914000000	-4.943997000000
C	-2.258579000000	-2.153112000000	-4.099422000000
C	-4.920204000000	-9.180116000000	-6.115376000000
C	-7.922874000000	-8.085692000000	-4.959914000000
C	-8.728482000000	-6.875293000000	-5.226642000000

C	-9.926248000000	-6.595341000000	-4.563837000000
C	-10.605483000000	-5.434421000000	-4.855537000000
C	-10.117955000000	-4.572404000000	-5.820790000000
C	-8.934135000000	-4.911171000000	-6.487186000000
C	-8.404246000000	-4.107216000000	-7.609785000000
C	-5.814589000000	-4.633554000000	-9.765014000000
C	-9.149447000000	-2.905456000000	-8.103584000000
C	-8.374671000000	-9.110520000000	-3.962476000000
C	-3.969515000000	-10.310825000000	-5.957638000000
C	-4.184423000000	-11.309154000000	-5.013713000000
C	-3.286837000000	-12.354200000000	-4.888180000000
C	-2.151277000000	-12.402072000000	-5.670798000000
C	-1.912179000000	-11.407529000000	-6.596829000000
C	-2.826433000000	-10.366077000000	-6.743829000000
C	-5.304369000000	-4.226344000000	-11.107629000000
C	-6.016680000000	-3.368410000000	-11.932277000000
C	-5.564079000000	-3.093137000000	-13.205201000000
C	-4.383549000000	-3.646340000000	-13.669559000000
C	-3.654083000000	-4.473139000000	-12.846685000000
C	-4.103688000000	-4.768592000000	-11.579127000000
C	-7.894965000000	-8.006282000000	-11.306276000000
C	-6.763140000000	-7.282341000000	-11.641738000000
C	-6.462133000000	-7.026467000000	-12.979124000000
C	-7.269604000000	-7.526606000000	-13.982829000000
C	-8.346095000000	-8.297719000000	-13.645555000000
C	-8.690005000000	-8.518747000000	-12.326070000000
C	-9.792754000000	-7.306539000000	-9.234687000000
C	-10.104684000000	-6.180825000000	-9.985760000000
C	-11.250071000000	-5.450765000000	-9.687663000000
C	-12.072135000000	-5.820583000000	-8.642061000000
C	-11.762055000000	-6.943434000000	-7.880259000000
C	-10.625411000000	-7.682245000000	-8.172996000000
C	-8.640479000000	-9.952248000000	-9.236193000000
C	-9.798910000000	-10.575985000000	-9.707220000000
C	-10.029748000000	-11.910184000000	-9.437507000000
C	-9.111011000000	-12.628848000000	-8.675314000000
C	-7.973094000000	-12.008684000000	-8.193569000000
C	-7.726460000000	-10.672044000000	-8.472215000000
H	4.292905000000	0.861523000000	-3.377360000000
H	5.526404000000	-1.235049000000	-2.856013000000
H	4.638284000000	-2.781546000000	-1.105989000000
H	4.180231000000	-3.262576000000	1.191363000000
H	3.179579000000	-4.313964000000	0.143735000000
H	2.617514000000	-3.924041000000	1.811701000000
H	1.659727000000	3.532571000000	-3.194498000000
H	2.377472000000	2.256674000000	-4.244407000000
H	3.387506000000	3.038732000000	-2.992498000000
H	-0.931696000000	4.822443000000	-2.798372000000
H	-2.541437000000	6.713322000000	-3.039760000000
H	-4.578400000000	6.801959000000	-1.627847000000

H	-5.006721000000	5.003512000000	0.042522000000
H	-3.354341000000	3.129654000000	0.292068000000
H	0.941824000000	-3.491338000000	4.374389000000
H	0.134525000000	-4.005090000000	6.677238000000
H	-1.984005000000	-3.010120000000	7.506978000000
H	-3.307706000000	-1.521601000000	6.021402000000
H	-2.466548000000	-0.986956000000	3.730449000000
H	-2.932482000000	-3.703452000000	-1.154527000000
H	-4.354473000000	-5.119601000000	-2.706480000000
H	0.090501000000	0.472644000000	3.664874000000
H	-0.434558000000	-0.015146000000	6.034732000000
H	1.017230000000	0.897960000000	7.858176000000
H	2.970354000000	2.296768000000	7.255202000000
H	3.572101000000	2.685970000000	4.914960000000
H	3.435079000000	-0.563597000000	3.630863000000
H	5.480970000000	-1.864984000000	3.112757000000
H	6.961252000000	-1.196476000000	1.233273000000
H	6.393332000000	0.812939000000	-0.140310000000
H	4.361474000000	2.139504000000	0.389153000000
H	4.533064000000	3.568034000000	3.092222000000
H	4.929902000000	5.968892000000	2.629573000000
H	3.283843000000	7.261187000000	1.269256000000
H	1.239893000000	6.139064000000	0.395903000000
H	0.818116000000	3.742087000000	0.892540000000
H	-3.081010000000	-2.725866000000	-6.026147000000
H	-1.659019000000	-1.309717000000	-4.474194000000
H	-10.306397000000	-7.290841000000	-3.803314000000
H	-11.539896000000	-5.194269000000	-4.324661000000
H	-10.651776000000	-3.647772000000	-6.074685000000
H	-10.193722000000	-3.166742000000	-8.372038000000
H	-9.193072000000	-2.115354000000	-7.324409000000
H	-8.631005000000	-2.505277000000	-8.992375000000
H	-7.673219000000	-9.961889000000	-3.986176000000
H	-8.390964000000	-8.685992000000	-2.936267000000
H	-9.400998000000	-9.468049000000	-4.188176000000
H	-5.081796000000	-11.251761000000	-4.382302000000
H	-3.472055000000	-13.142640000000	-4.140914000000
H	-1.435092000000	-13.231277000000	-5.552827000000
H	-1.006771000000	-11.432830000000	-7.223196000000
H	-2.659151000000	-9.558972000000	-7.472742000000
H	-6.955316000000	-2.937979000000	-11.555063000000
H	-6.148017000000	-2.424228000000	-13.857912000000
H	-4.029487000000	-3.419198000000	-14.687652000000
H	-2.705786000000	-4.907717000000	-13.202076000000
H	-3.546944000000	-5.442362000000	-10.911123000000
H	-6.103993000000	-6.901962000000	-10.845548000000
H	-5.578934000000	-6.414172000000	-13.215406000000
H	-7.030722000000	-7.327278000000	-15.038850000000
H	-8.983846000000	-8.726086000000	-14.435876000000
H	-9.585593000000	-9.115288000000	-12.095634000000

H	-9.448571000000	-5.865721000000	-10.811537000000
H	-11.494462000000	-4.564334000000	-10.293431000000
H	-12.974744000000	-5.232842000000	-8.413947000000
H	-12.406824000000	-7.242257000000	-7.040364000000
H	-10.374966000000	-8.568822000000	-7.569827000000
H	-10.546556000000	-9.997352000000	-10.272896000000
H	-10.943394000000	-12.398210000000	-9.810247000000
H	-9.297335000000	-13.690505000000	-8.449930000000
H	-7.253385000000	-12.568382000000	-7.576577000000
H	-6.831608000000	-10.171405000000	-8.073214000000

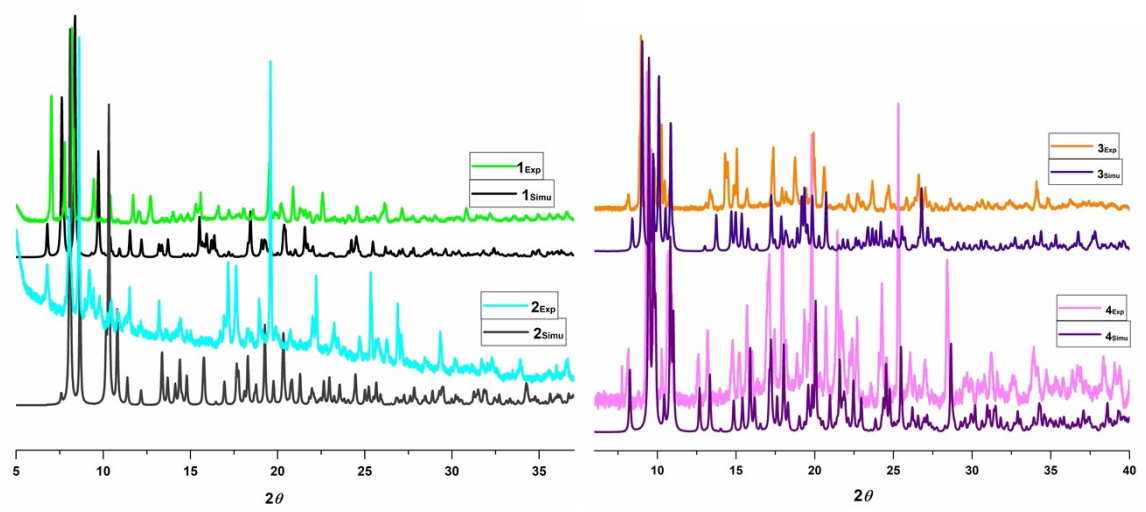

(a) **(b)**

Figure S31. Experimental powder XRD pattern and simulated powder XRD from single crystal data of (a) complex **1-2,** (b) complex **3-4**.

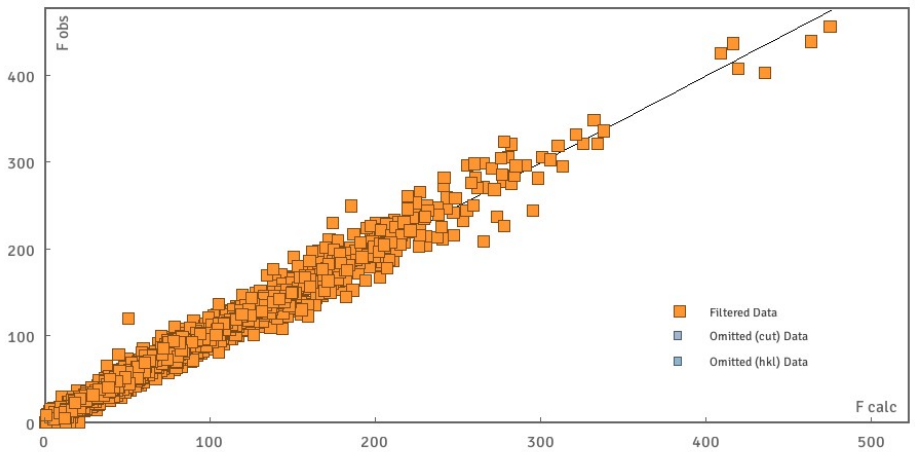

Figure S32. F_{obs} vs F_{calc} plot of complex **2**.

References

1. A. K. Bar, P. Kalita, J.-P. Sutter and V. Chandrasekhar, *Inorg. Chem.*, 2018, **57**, 2398-2401.
2. P. Kalita, N. Ahmed, A. K. Bar, S. Dey, A. Jana, G. Rajaraman, J.-P. Sutter and V. Chandrasekhar, *Inorg. Chem.*, 2020, **59**, 6603-6612.
3. P. Kalita, N. Ahmed, S. Moorthy, V. Béreau, A. K. Bar, P. Kumar, P. Nayak, J.-P. Sutter, S. K. Singh and V. Chandrasekhar, *Dalton Trans.*, 2023, **52**, 2804-2815.